

Loop Equation and Exact Soft Anomalous Dimension in $\mathcal{N} = 4$ Super Yang-Mills

Simone Giombi[♣], Shota Komatsu[◇]

[♣]*Department of Physics, Princeton University, Princeton, NJ 08544, USA*

[◇]*School of Natural Sciences, Institute for Advanced Study, Princeton, NJ 08540, USA*

sgiombi AT princeton.edu, skomatsu AT ias.edu

Abstract

BPS Wilson loops in supersymmetric gauge theories have been the subjects of active research since they are often amenable to exact computation. So far most of the studies have focused on loops that do not intersect. In this paper, we derive exact results for intersecting 1/8 BPS Wilson loops in $\mathcal{N} = 4$ supersymmetric Yang-Mills theory, using a combination of supersymmetric localization and the loop equation in 2d gauge theory. The result is given by a novel matrix-model-like representation which couples multiple contour integrals and a Gaussian matrix model. We evaluate the integral at large N , and make contact with the string world-sheet description at strong coupling. As an application of our results, we compute exactly a small-angle limit (and more generally near-BPS limits) of the cross anomalous dimension which governs the UV divergence of intersecting Wilson lines. The same quantity describes the soft anomalous dimension of scattering amplitudes of W -bosons in the Coulomb branch.

Contents

1	Introduction	3
2	1/8 BPS Wilson Loop, 2d YM and Matrix Model	5
2.1	1/8 BPS Wilson loops and matrix model	5
2.2	A new integral representation for Wilson loop correlators	7
2.2.1	A single fundamental loop	8
2.2.2	Multiple fundamental loops	10
3	Loop Equation and Intersecting Wilson Loops	13
3.1	Review of loop equation in 2d YM	14
3.2	Intersecting BPS loops in $\mathcal{N} = 4$ SYM	18
3.2.1	Figure eight loop	19
3.2.2	Two-intersection loop	23
4	Cross Anomalous Dimension at Small Angle	26
4.1	Cross anomalous dimension in $\mathcal{N} = 4$ SYM	26
4.2	Two-point function of intersections	28
4.3	Cross anomalous dimension from localization	30
4.4	U(1) factor and weak- and strong-coupling expansions	33
5	Conclusion	35
A	Infinite Sum of Modified Bessel Functions	37
B	Cross Anomalous Dimension of Two Touching Lines	38

1 Introduction

The loop equation was proposed initially in [1, 2] as an alternative way to formulate, and possibly solve, the gauge theories (see e.g. [3] for a review). It has the conceptual advantage that it directly constrains the most basic observables, namely the Wilson loops. In lower-dimensional theories such as matrix models [4] and two-dimensional Yang-Mills theory [5–8], it has proven to be a powerful tool for solving the theories exactly. Unfortunately, solving the loop equation is much harder in higher dimensions and progress remains to be made.

In this paper we demonstrate the power of the loop equation in higher dimensions when used in conjunction with other non-perturbative techniques. Specifically, we consider intersecting 1/8-BPS Wilson loops in $\mathcal{N} = 4$ supersymmetric Yang-Mills ($\mathcal{N} = 4$ SYM) and compute their expectation values at finite coupling and finite N using a combination of the loop equation and supersymmetric localization [9, 10].

The 1/8-BPS Wilson loop is a supersymmetric Wilson loops in $\mathcal{N} = 4$ SYM which can be defined on an arbitrary contour on a two-sphere and preserves four fermionic charges. It was conjectured in [11, 12] and later supported by supersymmetric localization [10] that its expectation value (as well as general correlation functions of any number of loops) coincides with that of the standard Wilson loop in two-dimensional Yang-Mills theory (2d YM) in a zero-instanton sector. Based on this, the expectation value of a non-intersecting 1/8-BPS loop was computed in [11, 12] generalizing the famous result for the 1/2-BPS loop [9, 13, 14]. It was also used to derive multi-matrix models for correlators of local operators and non-intersecting BPS loops [15, 16]. By now these results have been tested by numerous direct computations [17–22] and they provide convincing evidence for the equivalence between the BPS sector of $\mathcal{N} = 4$ SYM and 2d YM.

The goal of this paper is to generalize them to intersecting loops. The strategy is simple: Using the conjecture above, we relate the intersecting 1/8-BPS loops in $\mathcal{N} = 4$ SYM to intersecting Wilson loops in 2d YM on S^2 in the zero-instanton sector. We then solve the loop equation of 2d YM exactly at finite N . The loop equation in 2d YM was first solved for loops on R^2 at large N [5]. The result was generalized to loops on R^2 at finite N in [6] and to loops on S^2 at large N in [7, 8]. While all these results take simple and compact forms, no such expressions were known for loops on S^2 at finite N : the only known expression in the literature involves a rather complicated sum over the Young diagrams [23]. We show that a simple closed-form expression does exist for loops on S^2 at finite N if the theory is restricted to the zero-instanton sector—the sector relevant for the BPS loops in $\mathcal{N} = 4$ SYM.

The result of our computation is a coupled system of multiple integrals and a Gaussian matrix model. For instance, the expectation value of the *figure eight* loop with areas \bar{A}_1 and \bar{A}_2 reads (see figure 1)

$$\langle \mathcal{W}_{\text{figure-eight}} \rangle = \frac{i}{\pi\lambda} \oint_{\mathcal{C}_1 < \mathcal{C}_2} du_1 du_2 \frac{u_1 - u_2}{(u_1 - u_2)^2 + \left(\frac{\lambda}{4\pi N}\right)^2} \langle f_{4\pi - \bar{A}_1}(u_1) f_{\bar{A}_2}(u_2) \rangle_M. \quad (1.1)$$

Here $\lambda := g_{\text{YM}}^2 N$ is the 't Hooft coupling constant and the function f_A is defined by

$$f_A(u) := e^{iA(u - \frac{i\lambda}{8\pi N})} \frac{\det\left(u - M - \frac{i\lambda}{4\pi N}\right)}{\det(u - M)}, \quad (1.2)$$



Figure 1: (a) The figure eight Wilson loop with areas \bar{A}_1 and \bar{A}_2 . (b) Two intersecting lines (left) and two touching lines (right) which mix under the renormalization group flow.

while $\langle \bullet \rangle_M$ denotes the expectation value of \bullet in the Gaussian matrix model of size N ,

$$\langle \bullet \rangle_M := \frac{\int [dM] \bullet \exp \left[-\frac{8\pi^2}{g_{\text{YM}}^2} \text{tr}(M^2) \right]}{\int [dM] \exp \left[-\frac{8\pi^2}{g_{\text{YM}}^2} \text{tr}(M^2) \right]}. \quad (1.3)$$

The integration contours $\mathcal{C}_{1,2}$ encircle the eigenvalues of the Gaussian matrix model (1.3) and they are placed far apart from each other (see sections 2 and 3 for more details). The integral can be evaluated explicitly at large N and it gives

$$\langle \mathcal{W}_{\text{figure-eight}} \rangle \stackrel{N \rightarrow \infty}{=} \frac{\mathcal{I}_0^{\bar{a}_1} \mathcal{I}_1^{\bar{a}_2}}{2\pi g_{\bar{a}_2}} + \sum_{k=1}^{\infty} \frac{\rho_{\bar{a}_1}^k \mathcal{I}_k^{\bar{a}_1}}{4\pi g} \left[\left(\rho_{\bar{a}_2}^{k+1} + \frac{(-1)^k}{\rho_{\bar{a}_2}^{k+1}} \right) \mathcal{I}_{k+1}^{\bar{a}_2} + \left(\rho_{\bar{a}_2}^{k-1} + \frac{(-1)^k}{\rho_{\bar{a}_2}^{k-1}} \right) \mathcal{I}_{k-1}^{\bar{a}_2} \right],$$

where

$$g := \frac{\sqrt{\lambda}}{4\pi}, \quad \bar{a}_i := \frac{\bar{A}_i - 2\pi}{2}, \quad g_{\bar{a}} := g \sqrt{1 - \frac{\bar{a}^2}{\pi^2}}, \quad \rho_{\bar{a}} := \sqrt{\frac{\pi + \bar{a}}{\pi - \bar{a}}}, \quad (1.4)$$

and $\mathcal{I}_k^{\bar{a}} := I_k(4\pi g_{\bar{a}})$ is the modified Bessel function. The result at strong coupling reproduces the area of the minimal surface as we show in section 3.2.1.

As an important application, we compute a small angle limit of the *cross anomalous dimension* of intersecting Wilson lines. The cross anomalous dimension controls the mixing of two different configurations of Wilson lines, two intersecting lines and two touching lines (see figure 1), under the renormalization group. It also describes the *soft anomalous dimension*, which controls how the soft gluons transfer the color degrees of freedom of partons in a scattering process. We generalize the analysis of the Bremsstrahlung function in [24, 25] and relate the small angle limit—and more generally the near-BPS limits—of these anomalous dimensions to our localization computations. The results are exact at finite λ and N and reproduce the answers at weak coupling in the literature [26–28].

The formalism in this paper will be used in our upcoming paper [29] on the defect CFT correlators on the higher-rank Wilson loops. There, we consider a configuration in which multiple fundamental Wilson loops with different areas are joined together by a projector to a higher-rank representation. We compute its expectation value by taking an appropriate linear combination of multiply intersecting loops.

The rest of the paper is organized as follows. In section 2, we review the 1/8 BPS Wilson loops and their relation to 2d YM. We then present a new integral representation for

correlators of non-intersecting Wilson loops which simplifies the analysis of the loop equation in the subsequent sections. In section 3, we review the loop equation in 2d YM and solve it in the zero-instanton sector on S^2 . As a result, we obtain a closed-form integral representation for intersecting loops. We then demonstrate how to evaluate the integral at large N using examples of a figure eight loop and a two-intersection loop and study the weak- and strong-coupling limits. In section 4, we use these results to compute the small-angle and near-BPS limits of the cross anomalous dimension at finite λ and N . We then discuss future directions in section 5. A few appendices are provided to explain technical details.

2 1/8 BPS Wilson Loop, 2d YM and Matrix Model

2.1 1/8 BPS Wilson loops and matrix model

In supersymmetric gauge theories, one can often define a supersymmetric generalization of the Wilson loop by coupling the loop to scalar fields. The 1/8 BPS Wilson loop in $\mathcal{N} = 4$ SYM is a special kind of such operators which can be defined for an arbitrary contour C on S^2 inside R^4 or S^4 (see figure 2):

$$\mathcal{W}_{1/8} := \frac{1}{N} \text{tr} \text{Pexp} \left(\oint_C (iA_j + \epsilon_{kjl} x^k \Phi^l) dx^j \right). \quad (2.1)$$

Here all the indices run from 1 to 3 and x^j 's are the coordinates of S^2 , $\sum_{j=1}^3 (x^j)^2 = 1$. Throughout this paper, we consider the $U(N)$ gauge group unless otherwise stated.

It was conjectured through the perturbative computations [11, 12] and later supported by the localization [10] that the computation of the 1/8 BPS Wilson loop reduces to that of the standard Wilson loop in 2d YM on S^2 in the zero-instanton sector,

$$\mathcal{W}_{1/8} \longleftrightarrow \mathcal{W}_{2\text{dYM}} := \frac{1}{N} \text{tr} \text{Pexp} \left(\oint_C iA_j dx^j \right), \quad (2.2)$$

where the coupling constants of 2d YM (g_{2d}) and $\mathcal{N} = 4$ SYM (g_{YM}) are related by

$$g_{2d}^2 = -\frac{g_{\text{YM}}^2}{2\pi}, \quad (2.3)$$

and the action of 2d YM is

$$S_{2d} = \frac{1}{g_{2d}^2} \int d^2\sigma \sqrt{g} \text{tr} (F_{\mu\nu} F^{\mu\nu}). \quad (2.4)$$

The expectation value of a single 1/8-BPS loop was computed by resumming the perturbative series in 2d YM and re-expressing it as a matrix integral¹,

$$\langle \mathcal{W}_{1/8} \rangle = \frac{1}{Z} \int [d\Phi] \frac{1}{N} \text{tr} (e^\Phi) e^{-\frac{(4\pi)^2}{2A(4\pi-A)g_{\text{YM}}^2} \text{tr}(\Phi^2)}. \quad (2.5)$$

¹ Z is a partition function of the matrix model, namely a matrix integral without the insertion of $\text{tr}(e^\Phi)/N$.

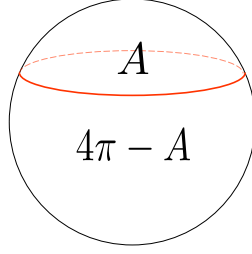


Figure 2: The 1/8-BPS Wilson loop on S^2 . The 1/8-BPS loop can be defined on an arbitrary contour on S^2 and its coupling to scalars is given by (2.1). A single loop divides S^2 into two regions, one with area A and the other with area $4\pi - A$. Its expectation value depends only on the area A owing to the relation to 2d YM.

By evaluating this matrix integral, we get

$$\langle \mathcal{W}_{1/8} \rangle = \frac{1}{N} L_{N-1}^1 \left(-\frac{\lambda'}{4N} \right) e^{\frac{\lambda'}{8N}}, \quad \lambda' := \lambda \left(1 - \frac{(A - 2\pi)^2}{4\pi^2} \right), \quad (2.6)$$

where $\lambda := g_{\text{YM}}^2 N$ is the 't Hooft coupling constant, L_{N-1}^1 is an associated Laguerre polynomial and A is the area of the region encircled by the Wilson loop. The large N limit of this result gives a generalization of the famous result for the 1/2-BPS Wilson loop,

$$\langle \mathcal{W}_{1/8} \rangle \stackrel{N \rightarrow \infty}{\simeq} \frac{2}{\sqrt{\lambda'}} I_1(\sqrt{\lambda'}), \quad (2.7)$$

with I_n being the modified Bessel function.

As another application of the relation (2.2), a multi-matrix model for the correlation functions of 1/8-BPS Wilson loops was derived in [16]. A heuristic way² to derive the matrix model is as follows: First we rewrite the action of 2d YM as a deformed BF theory,

$$S = \int \text{tr}(B \wedge F) - \frac{g_{2d}^2}{4} \int d^2\sigma \sqrt{g} \text{tr}(B^2). \quad (2.8)$$

If one integrates out B , one recovers the standard 2d YM action. Second we use the fact that the theory reduces essentially to the abelian theory and localizes to configurations for which B is piecewise constant with discontinuities across the Wilson loops. In such configurations, the first term of the action (2.8) becomes a boundary term

$$\int_{\Sigma} \text{tr}(B \wedge F) = \text{tr} \left[B \int_{\partial\Sigma} A \right] = -i \text{tr}[BX], \quad (2.9)$$

where Σ is a subregion of S^2 whose boundaries are given by the Wilson loops and $X := i \int_{\partial\Sigma} A$ is a boundary holonomy. On the other hand the second term simply gives

$$-\frac{g_{2d}^2}{4} \int_{\Sigma} d^2\sigma \sqrt{g} \text{tr}(B^2) = -\frac{g_{2d}^2 A_{\Sigma}}{4} \text{tr}(B^2) = \frac{g_{\text{YM}}^2 A_{\Sigma}}{8\pi} \text{tr}(B^2), \quad (2.10)$$

²See [16] for more rigorous discussions.

where A_Σ is the area of the region Σ .

Performing such rewritings to each region Σ_m , we obtain the following multi-matrix model action:

$$\hat{S} = \sum_{\{\Sigma_m\}} \left[-i \text{tr} \left(\sum_{j \in \partial \Sigma_m} s_j^{(m)} \hat{B}_{\Sigma_m} \hat{X}_j \right) + \frac{g_{\text{YM}}^2 A_{\Sigma_m}}{8\pi} \text{tr} \left(\hat{B}_{\Sigma_m}^2 \right) \right]. \quad (2.11)$$

Here $s_j^{(m)}$ is an orientation factor which takes value $+1$ when the holonomy \hat{X}_j is oriented in the same direction as the boundary $\partial \Sigma_m$, and -1 otherwise. From this action, the correlator of the Wilson loops can be computed as follows,

$$\left\langle \prod_k \mathcal{W}_k \right\rangle = \frac{\int [d\hat{B}_{\Sigma_m}] [d\hat{X}_j] \prod_k \text{tr}_{r_k} (e^{\hat{X}_k}) e^{-\hat{S}}}{\int [d\hat{B}_{\Sigma_m}] [d\hat{X}_j] e^{-\hat{S}}}, \quad (2.12)$$

where r_k is the representation of the k -th Wilson loop \mathcal{W}_k . As was done in [16], one can integrate out \hat{B}_{Σ_m} 's and obtain an action purely in terms of \hat{X}_j 's. This however is not convenient for analyzing the loop equation since the resulting action depends nonlinearly on the areas A_{Σ_m} . In this paper, we instead integrate out \hat{X}_j and derive a new integral representation which is more convenient for the application of the loop equation.

2.2 A new integral representation for Wilson loop correlators

To derive an integral representation, it is convenient to first rescale the matrices as

$$X_j := \frac{4\pi \hat{X}_j}{g_{\text{YM}}^2}, \quad B_{\Sigma_m} := \frac{g_{\text{YM}}^2 \hat{B}_{\Sigma_m}}{4\pi}. \quad (2.13)$$

Then, the action and the correlator read

$$S = \sum_{\{\Sigma_m\}} \left[-i \text{tr} \left(\sum_{j \in \partial \Sigma_m} s_j^{(m)} B_{\Sigma_m} X_j \right) + \frac{2\pi A_{\Sigma_m}}{g_{\text{YM}}^2} \text{tr} (B_{\Sigma_m}^2) \right], \quad (2.14)$$

$$\left\langle \prod_k \mathcal{W}_k \right\rangle = \frac{\int [dB_{\Sigma_m}] [dX_j] \prod_k \text{tr}_{r_k} (e^{\epsilon X_k}) e^{-S}}{\int [dB_{\Sigma_m}] [dX_j] e^{-S}},$$

with

$$\epsilon := \frac{g_{\text{YM}}^2}{4\pi} = \frac{\lambda}{4\pi N} = \frac{4\pi g^2}{N}. \quad (2.15)$$

In the last equality, we used the notation for the 't Hooft coupling constant commonly used in the integrability literature,

$$g^2 := \frac{\lambda}{16\pi^2}. \quad (2.16)$$

2.2.1 A single fundamental loop

Let us first discuss the expectation value of a single fundamental Wilson loop with no self-intersections. In the presence of a Wilson loop, S^2 is divided into two regions, one with the area $4\pi - A(=: A_0)$ and the other with the area $A(=: A_1)$ (see figure 2), and the action of the matrix model reads

$$S = \frac{2\pi A_0}{g_{\text{YM}}^2} \text{tr}(B_0^2) + \frac{2\pi A_1}{g_{\text{YM}}^2} \text{tr}(B_1^2) - i \text{tr}(X(B_0 - B_1)) . \quad (2.17)$$

To compute the expectation value of the Wilson loop in this matrix model, we use the Harish-Chandra-Itzykson-Zuber identity

$$\int d\Omega e^{i \text{tr}(\Omega^\dagger A \Omega B)} = \frac{\det e^{i a_i b_j}}{\Delta(a) \Delta(b)} , \quad (2.18)$$

where A and B are diagonal matrices with entries a_j 's and b_j 's respectively, $\int d\Omega$ is an integral over the unitary matrices and Δ is the Vandermonde determinant $\Delta(a) := \prod_{i < j} (a_i - a_j)$.

Using (2.18), we can reduce the partition function of the matrix model (2.17) to integrals of eigenvalues,

$$Z = \int [dX][dB_0][dB_1] e^{-S} = \int d^N x d^N b^{(0)} d^N b^{(1)} \mathcal{I} , \quad (2.19)$$

where the integrand \mathcal{I} is given by

$$\begin{aligned} \mathcal{I} &= \Delta^2(x) \Delta^2(b^{(0)}) \Delta^2(b^{(1)}) \frac{\det e^{i x_i b_j^{(0)}} \det e^{-i x_k b_l^{(1)}}}{\Delta^2(x) \Delta(b^{(0)}) \Delta(b^{(1)})} e^{-\frac{2\pi}{g_{\text{YM}}^2} \sum_j (A_0 (b_j^{(0)})^2 + A_1 (b_j^{(1)})^2)} \\ &= \Delta(b^{(0)}) \Delta(b^{(1)}) \det e^{i x_i b_j^{(0)}} \det e^{-i x_k b_l^{(1)}} e^{-\frac{2\pi}{g_{\text{YM}}^2} \sum_j (A_0 (b_j^{(0)})^2 + A_1 (b_j^{(1)})^2)} . \end{aligned} \quad (2.20)$$

We next expand the determinants into a sum over permutations:

$$\det e^{i x_i b_j^{(0)}} = \sum_{\sigma \in S_N} (-1)^\sigma \prod_j e^{i x_i b_{\sigma_j}^{(0)}} , \quad \det e^{-i x_k b_l^{(1)}} = \sum_{\sigma' \in S_N} (-1)^{\sigma'} \prod_j e^{-i x_i b_{\sigma'_j}^{(1)}} . \quad (2.21)$$

Owing to the symmetry of the rest of the integrand, all these permutations give the same answer. We thus pick the simplest one ($\sigma_j = j$ and $\sigma'_j = j$) and multiply a factor $(N!)^2$. After integrating out x 's, we get

$$\begin{aligned} Z &= (2\pi)^N (N!)^2 \int \left(\prod_{s=0}^1 d^N b^{(s)} \Delta(b^{(s)}) \right) \left(\prod_k \delta(b_k^{(0)} - b_k^{(1)}) \right) e^{-\frac{2\pi}{g_{\text{YM}}^2} \sum_j (A_0 (b_j^{(0)})^2 + A_1 (b_j^{(1)})^2)} \\ &= (2\pi)^N (N!)^2 \int d^N b \Delta^2(b) e^{-\frac{8\pi^2}{g_{\text{YM}}^2} \sum_j (b_j)^2} . \end{aligned} \quad (2.22)$$

In the second line, we integrated out $b^{(1)}$'s and denoted the remaining variables $b_j^{(0)}$ as b_j . We also used $A_0 + A_1 = 4\pi$ to simplify the exponent.

Similarly, the expectation value of the fundamental Wilson loop can be reduced to the following eigenvalue integral:

$$\langle \mathcal{W} \rangle = \frac{1}{Z} \int [dX][dB_0][dB_1] \frac{\text{tr}(e^{\epsilon X})}{N} e^{-S} = \frac{1}{Z} \int d^N x d^N b^{(0)} d^N b^{(1)} \mathcal{I} \frac{\sum_k e^{\epsilon x_k}}{N}, \quad (2.23)$$

with \mathcal{I} defined in (2.20). To evaluate this integral, we again expand the determinants and integrate out x 's. The only modification is that one of the delta functions gets shifted by $-i\epsilon$ owing to the factor $e^{\epsilon x_k}$. We then get

$$\begin{aligned} \langle \mathcal{W} \rangle &= \frac{(2\pi)^N (N!)^2}{Z} \int \left(\prod_{s=0}^1 d^N b^{(s)} \Delta(b^{(s)}) \right) \sum_k \frac{\delta(b_k^{(0)} - b_k^{(1)} - i\epsilon)}{N} \\ &\quad \times \left(\prod_{j \neq k} \delta(b_j^{(0)} - b_j^{(1)}) \right) e^{-\frac{2\pi}{g_{\text{YM}}^2} \sum_j (A_0(b_j^{(0)})^2 + A_1(b_j^{(1)})^2)} \\ &= \frac{(2\pi)^N (N!)^2}{Z} \int d^N b \Delta^2(b) e^{-\frac{8\pi^2}{g_{\text{YM}}^2} \sum_j (b_j)^2} \frac{\sum_k e^{iA_1(b_k - \frac{i\epsilon}{2})} \prod_{j \neq k} \frac{b_k - b_j - i\epsilon}{b_k - b_j}}{N}. \end{aligned} \quad (2.24)$$

Now the crucial observation is that the sum \sum_k can be recast into a contour integral,

$$\langle \mathcal{W} \rangle = \frac{(2\pi)^N (N!)^2}{Z} \int d^N b \Delta^2(b) e^{-\frac{8\pi^2}{g_{\text{YM}}^2} \sum_j (b_j)^2} \left[\oint_{\mathcal{C}} \frac{du}{8\pi^2 g^2} e^{iA_1(u - \frac{i\epsilon}{2})} \prod_j \frac{u - b_j - i\epsilon}{u - b_j} \right]. \quad (2.25)$$

We can then interpret this as an expectation value of a Gaussian matrix model and get

$$\langle \mathcal{W} \rangle = \left\langle \oint_{\mathcal{C}} \frac{du}{8\pi^2 g^2} f_{A_1}(u) \right\rangle_M. \quad (2.26)$$

Here the integration contour \mathcal{C} encircles all the eigenvalues b_k 's and f_A is given by

$$f_A(u) := e^{iA(u - \frac{i\epsilon}{2})} \det \left[\frac{u - M - i\epsilon}{u - M} \right]. \quad (2.27)$$

The symbol $\langle \bullet \rangle_M$ denotes the expectation value of \bullet in a Gaussian matrix model with the action $S_M := 8\pi^2 \text{tr}(M^2) / g_{\text{YM}}^2$:

$$\langle \bullet \rangle_M := \frac{\int [dM] \bullet e^{-S_M}}{\int [dM] e^{-S_M}}. \quad (2.28)$$

The result (2.26) may appear more complicated than the expressions known in the literature [11, 12]. However, for the analysis of the loop equation, (2.26) is more convenient since the area-dependence is simple. See section 3 for more details.

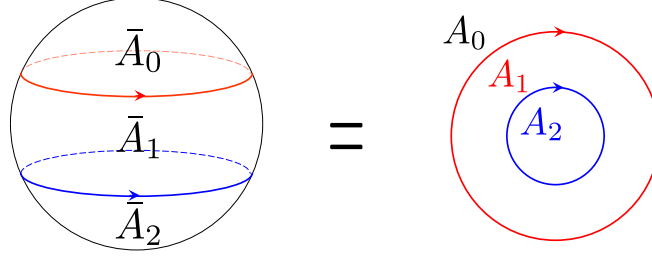


Figure 3: Two 1/8-BPS loops with the same orientations. Left: The loops divide S^2 into three disconnected regions with areas \bar{A}_0 , \bar{A}_1 and \bar{A}_2 . Right: The same configuration viewed from the south pole. We denote the areas inside outer (red) and inner (blue) circles by A_1 and A_2 respectively and the area of the complement by A_0 . The two sets of areas are related by $\bar{A}_0 = A_0$, $\bar{A}_1 = A_1 - A_2$ and $\bar{A}_2 = A_2$.

2.2.2 Multiple fundamental loops

We now generalize the result (2.26) to correlators of multiple Wilson loops.

To see how it works, let us first consider the correlator of two fundamental Wilson loops with the same orientation. As depicted in figure 3, we denote the areas inside outer and inner loops by A_1 and A_2 respectively and the area of the complement by A_0 . Then the matrix model action is given by

$$S = \sum_{s=0}^2 \frac{2\pi \bar{A}_s}{g_{\text{YM}}^2} \text{tr}(B_s^2) - i \sum_{s=1,2} \text{tr}(X_s(B_{s-1} - B_s)) , \quad (2.29)$$

with $\bar{A}_0 := A_0$, $\bar{A}_1 := A_1 - A_2$ and $\bar{A}_2 := A_2$. By reducing the matrix integral to the eigenvalues using the identity (2.18), we get

$$Z = \int \left(\prod_{s=0}^2 [dB_s] \right) \left(\prod_{s=1,2} [dX_s] \right) e^{-S} = \int \left(\prod_{s=0}^2 d^N b^{(s)} \right) \left(\prod_{s=1,2} d^N x^{(s)} \right) \mathcal{I}_2 , \quad (2.30)$$

with

$$\mathcal{I}_2 = \Delta(b^{(0)})\Delta(b^{(2)}) \left(\prod_{s=1}^2 \det e^{ix_i^{(s)} b_j^{(s-1)}} \det e^{-ix_i^{(s)} b_j^{(s)}} \right) e^{-\frac{2\pi}{g_{\text{YM}}^2} \sum_{s=0}^2 \sum_j \bar{A}_s (b_j^{(s)})^2} \quad (2.31)$$

Expanding a product of determinants, we obtain a sum of permutations

$$\prod_{s=1}^2 \det e^{ix_i^{(s)} b_j^{(s-1)}} \det e^{-ix_i^{(s)} b_j^{(s)}} = \sum_{\sigma^0, \sigma^1, \sigma^2, \sigma^3} (-1)^{\sum_s \sigma^s} \prod_j e^{i(b_{\sigma_j^0}^{(0)} - b_{\sigma_j^1}^{(1)})x_j^{(1)}} e^{i(b_{\sigma_j^1}^{(1)} - b_{\sigma_j^2}^{(2)})x_j^{(2)}} . \quad (2.32)$$

Again all these permutations turn out to give the same result owing to the symmetry of the integrand. We can therefore replace the integrand \mathcal{I}_2 with

$$\mathcal{I}_2 = (N!)^4 \Delta(b^{(0)})\Delta(b^{(2)}) \left(\prod_j e^{i(b_j^{(0)} - b_j^{(1)})x_j^{(1)}} e^{i(b_j^{(1)} - b_j^{(2)})x_j^{(2)}} \right) e^{-\frac{2\pi}{g_{\text{YM}}^2} \sum_{s=0}^2 \sum_j \bar{A}_s (b_j^{(s)})^2} . \quad (2.33)$$

Plugging this expression into (2.30), we find that the integrals of $x_j^{(k)}$ give the delta functions $\delta(b_j^{(0)} - b_j^{(1)})$ and $\delta(b_j^{(1)} - b_j^{(2)})$. Performing the integrals of $b^{(1)}$ and $b^{(2)}$, we get

$$Z = (2\pi)^{2N} (N!)^4 \int d^N b \Delta^2(b) e^{-\frac{8\pi^2}{g_{\text{YM}}^2} \sum_j (b_j)^2}. \quad (2.34)$$

Here we again denoted $b_j^{(0)}$ by b_j and used $\sum_s A_s = 4\pi$.

To compute the correlator of the Wilson loops, we insert

$$\frac{1}{N^2} \text{tr}(e^{\epsilon X_1}) \text{tr}(e^{\epsilon X_2}) \mapsto \frac{1}{N^2} \sum_{n,m} e^{\epsilon x_n^{(1)} + \epsilon x_m^{(2)}}, \quad (2.35)$$

to the partition function (2.30). We then obtain

$$\begin{aligned} \langle \mathcal{W}_1 \mathcal{W}_2 \rangle &= \frac{(2\pi)^{2N} (N!)^4}{Z} \int \left(\prod_{s=0}^2 d^N b^{(s)} \right) \Delta(b^{(0)}) \Delta(b^{(2)}) e^{-\frac{2\pi}{g_{\text{YM}}^2} \sum_{s=0}^2 \sum_j \bar{A}_s (b_j^{(s)})^2} \\ &\times \sum_{n,m} \frac{\delta(b_n^{(0)} - b_n^{(1)} - i\epsilon) \delta(b_m^{(1)} - b_m^{(2)} - i\epsilon)}{N^2} \prod_{\substack{j \neq n \\ k \neq m}} \delta(b_j^{(0)} - b_j^{(1)}) \delta(b_k^{(1)} - b_k^{(2)}). \end{aligned} \quad (2.36)$$

To proceed, we split the sum into two parts,

$$\sum_{n,m} = \sum_{n \neq m} + \sum_{n=m}, \quad (2.37)$$

integrate out $b_j^{(1,2)}$'s and recast the sums into integrals. The first term in (2.37) gives

$$\begin{aligned} \langle \mathcal{W}_1 \mathcal{W}_2 \rangle_{n \neq m} &= \frac{(2\pi)^{2N} (N!)^4}{Z} \int d^N b \Delta^2(b) e^{-\frac{8\pi^2}{g_{\text{YM}}^2} \sum_j (b_j)^2} \sum_{n \neq m} \frac{e^{iA_1(b_n - \frac{i\epsilon}{2})} e^{iA_2(b_m - \frac{i\epsilon}{2})}}{N^2} \\ &\times \frac{(b_n - b_m)^2}{(b_n - b_m)^2 + \epsilon^2} \prod_{j \neq n} \frac{b_n - b_j - i\epsilon}{b_n - b_j} \prod_{k \neq m} \frac{b_m - b_k - i\epsilon}{b_m - b_k}, \\ &= \frac{(2\pi)^{2N} (N!)^4}{Z} \int d^N b \Delta^2(b) e^{-\frac{8\pi^2}{g_{\text{YM}}^2} \sum_j (b_j)^2} \oint_{\mathcal{C}} \frac{du_1 e^{iA_1(u_1 - \frac{i\epsilon}{2})}}{8\pi^2 g^2} \frac{du_2 e^{iA_2(u_2 - \frac{i\epsilon}{2})}}{8\pi^2 g^2} \\ &\times \bar{\Delta}(u_1, u_2) \prod_j \frac{u_1 - b_j - i\epsilon}{u_1 - b_j} \prod_k \frac{u_2 - b_k - i\epsilon}{u_2 - b_k}, \end{aligned} \quad (2.38)$$

where the “interaction term” $\bar{\Delta}(u, v)$ is given by

$$\bar{\Delta}(u, v) := \frac{(u - v)^2}{(u - v)^2 + \epsilon^2}. \quad (2.39)$$

Again (2.38) can be interpreted as an expectation value in the Gaussian matrix model

$$\langle \mathcal{W}_1 \mathcal{W}_2 \rangle_{n \neq m} = \left\langle \oint_{\mathcal{C}} \frac{du_1}{8\pi^2 g^2} \frac{du_2}{8\pi^2 g^2} \bar{\Delta}(u_1, u_2) f_{A_1}(u_1) f_{A_2}(u_2) \right\rangle_M. \quad (2.40)$$

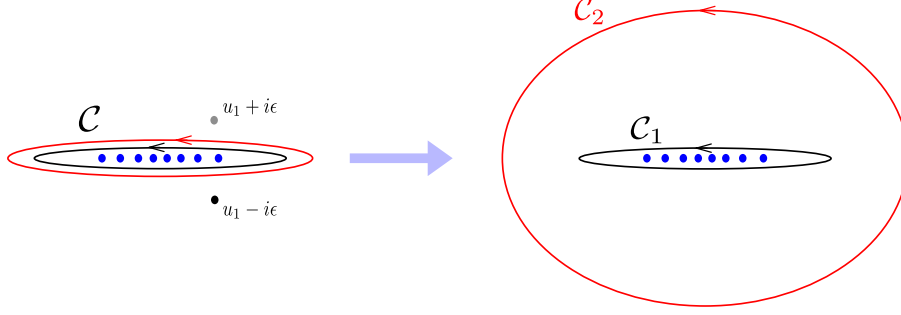


Figure 4: Deformation of the integration contours. Left: The integration contours for u_1 (black) and u_2 (red) in (2.42). The two contours are on top of each other and encircle the eigenvalues of M (the blue dots in the figure). Right: The integration contours in (2.46). When we deform the contour of u_2 , the integral picks up a contribution from poles at $u_2 = u_1 \pm i\epsilon$ (the gray and black dots). The residue at $u_1 + i\epsilon$ turns out to vanish while the residue at $u_1 - i\epsilon$ cancels the second term in (2.42).

Similarly, the second term in (2.37) gives³

$$\begin{aligned} \langle \mathcal{W}_1 \mathcal{W}_2 \rangle_{n=m} &= \frac{(2\pi)^{2N} (N!)^4}{Z} \int d^N b \Delta^2(b) e^{-\frac{8\pi^2}{g_{\text{YM}}^2} \sum_j (b_j)^2} \sum_n \frac{e^{iA_1(b_n - i\epsilon/2)} e^{iA_2(b_n - 3i\epsilon/2)}}{N^2} \\ &\quad \times \prod_{j \neq n} \frac{b_n - b_j - 2i\epsilon}{b_n - b_j} \\ &= \frac{1}{2N} \left\langle \oint_{\mathcal{C}} \frac{du}{8\pi^2 g^2} f_{A_1}(u) f_{A_2}(u - i\epsilon) \right\rangle_M. \end{aligned} \quad (2.41)$$

Thus the sum of the two contributions (2.40) and (2.41) gives

$$\begin{aligned} \langle \mathcal{W}_1 \mathcal{W}_2 \rangle &= \\ &\left\langle \oint_{\mathcal{C}} \frac{du_1}{8\pi^2 g^2} \frac{du_2}{8\pi^2 g^2} \bar{\Delta}(u_1, u_2) f_{A_1}(u_1) f_{A_2}(u_2) \right\rangle_M + \frac{1}{2N} \left\langle \oint_{\mathcal{C}} \frac{du}{8\pi^2 g^2} f_{A_1}(u) f_{A_2}(u - i\epsilon) \right\rangle_M. \end{aligned} \quad (2.42)$$

One can further simplify the expression by combining the two terms in (2.42): In the first term of (2.42), the integration contours of $u_{1,2}$ are on top of each other and encircle all the eigenvalues of the matrix model (see figure 4). If one deforms the contour of u_2 so that the two contours are far separated, the integral picks up a contribution from poles in the interaction term

$$\bar{\Delta}(u_1, u_2) = \frac{(u_1 - u_2)^2}{(u_1 - u_2)^2 + \epsilon^2}, \quad (2.43)$$

whose residues are

$$(\text{Residue at } u_2 = u_1 \pm i\epsilon) = \pm \frac{1}{2N} \left\langle \oint_{\mathcal{C}} \frac{du}{8\pi^2 g^2} f_{A_1}(u) f_{A_2}(u \pm i\epsilon) \right\rangle_M \quad (2.44)$$

³The term (2.41) resembles the “bound-state” contribution in the hexagon approach to the correlation functions [30, 31]. See also the comments below (2.47).

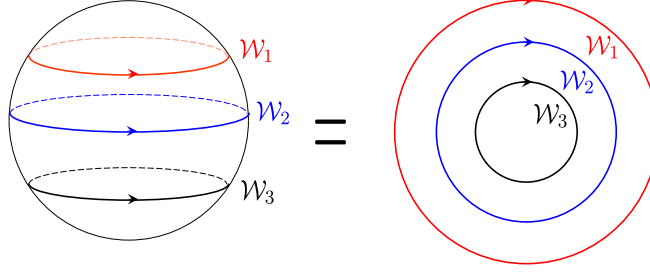


Figure 5: Multiple 1/8-BPS loops with the same orientations. The left figure is a configuration drawn on S^2 while the right figure is the same configuration viewed from the south pole and projected to a plane. We denote the area inside \mathcal{W}_j (in the right figure) by A_j .

The residue at $u_2 = u_1 + i\epsilon$ turns out to vanish since the product $f_{A_1}(u)f_{A_2}(u + i\epsilon)$ is

$$f_{A_1}(u)f_{A_2}(u + i\epsilon) \propto \det \frac{u - M - i\epsilon}{u - M} \det \frac{u - M}{u - M + i\epsilon} = \det \frac{u - M - i\epsilon}{u - M + i\epsilon}, \quad (2.45)$$

which is nonsingular inside the integration contour \mathcal{C} . On the other hand, the residue at $u_2 = u_1 - i\epsilon$ precisely cancels the second term in (2.42). We therefore arrive at the following simple expression for the correlator of two fundamental loops:

$$\langle \mathcal{W}_1 \mathcal{W}_2 \rangle = \left\langle \oint_{\mathcal{C}_1 \prec \mathcal{C}_2} \frac{du_1}{8\pi^2 g^2} \frac{du_2}{8\pi^2 g^2} \bar{\Delta}(u_1, u_2) f_{A_1}(u_1) f_{A_2}(u_2) \right\rangle_M. \quad (2.46)$$

The notation $\mathcal{C}_1 \prec \mathcal{C}_2$ means that the contour \mathcal{C}_1 is inside the contour \mathcal{C}_2 and they are far separated from each other.

Carrying out the same analysis for correlators of more than two Wilson loops of the same orientations (see figure 5 for details of the setup), we obtain a simple generalization of (2.46),

$$\left\langle \prod_{j=1}^n \mathcal{W}_j \right\rangle = \left\langle \oint_{\mathcal{C}_1 \prec \dots \prec \mathcal{C}_n} \prod_{j=1}^n \frac{du_j f_{A_j}(u_j)}{8\pi^2 g^2} \prod_{j < k} \bar{\Delta}(u_j, u_k) \right\rangle_M. \quad (2.47)$$

Interestingly this integral resembles multiparticle integrals [30–40] in the hexagon approach to the correlation functions and we will use this connection in our upcoming paper [29] to analyze the defect CFT correlators on the higher-rank Wilson loop.

3 Loop Equation and Intersecting Wilson Loops

We now discuss intersecting 1/8 BPS Wilson loops. In section 3.1, we review the derivation of the loop equation in 2d YM in [5]. We then apply it to the results in the previous section and derive integral representations for the intersecting BPS Wilson loops in section 3.2.

Let us make a remark before we proceed: Below we consider the Wilson loops without the normalization factor $1/N$ since they are often more convenient for analyzing the loop equation. To distinguish them from a more standard definition (2.2), we will put a tilde as

$$\tilde{\mathcal{W}}_{\mathcal{C}} := \text{tr} \text{Pe}^{i \oint_{\mathcal{C}} A_{\mu} dy^{\mu}}. \quad (3.1)$$



Figure 6: (a) Deformation of the contour $\delta\mathcal{C}_x$ denoted in red. We pick a point x close to the Wilson loop, draw a small circle and connect it to the original contour. (b) One-loop correction to $\langle \text{Sym} \rangle$ coming from the gluon exchange. Here we used the double-line notation to make manifest the contraction of indices.

3.1 Review of loop equation in 2d YM

We consider an infinitesimal deformation of the contour $\mathcal{C} \rightarrow \mathcal{C} + \delta\mathcal{C}_x$. Specifically, we pick a point x close to but *not* on top of the Wilson loop. We then add a small circle around x and connect it the original contour as depicted in figure 6. This defines the *area derivative*

$$\frac{\delta \langle \tilde{\mathcal{W}}_{\mathcal{C}} \rangle}{\delta \sigma^{\mu\nu}(x)} := \lim_{\delta \sigma^{\mu\nu} \rightarrow 0} \frac{\langle \tilde{\mathcal{W}}_{\mathcal{C} + \delta\mathcal{C}_x} \rangle - \langle \tilde{\mathcal{W}}_{\mathcal{C}} \rangle}{\delta \sigma^{\mu\nu}}. \quad (3.2)$$

Here $\delta \sigma^{\mu\nu}$ is an *area tensor* of $\delta\mathcal{C}_x$, which is a product of the area $|\delta\sigma|$ and the *orientation tensor* $n^{\mu\nu}$:

$$\delta \sigma^{\mu\nu} := |\delta\sigma| n^{\mu\nu}. \quad (3.3)$$

The orientation tensor is unit-normalized and parameterizes the orientation of $\delta\mathcal{C}_x$,

$$\frac{1}{2} n_{\mu\nu} n^{\mu\nu} = 1, \quad |\delta\sigma| = \frac{1}{2} n_{\mu\nu} \delta \sigma^{\mu\nu}. \quad (3.4)$$

We then expand the path-ordered exponential to get

$$\begin{aligned} \langle \tilde{\mathcal{W}}_{\mathcal{C} + \delta\mathcal{C}_x} \rangle - \langle \tilde{\mathcal{W}}_{\mathcal{C}} \rangle &= \left\langle \text{trP} \left[\left(e^{\oint_{\delta\mathcal{C}_x} i A_{\mu} dy^{\mu}} - 1 \right) e^{\oint_{\mathcal{C}} i A_{\mu} dy^{\mu}} \right] \right\rangle \\ &= \left\langle \text{trP} \left[\left(\oint_{\delta\mathcal{C}_x} i A_{\mu} dy^{\mu} - \frac{1}{2} \oint_{\delta\mathcal{C}_x \times \delta\mathcal{C}_x} A_{\mu}(y_1) A_{\nu}(y_2) dy_1^{\mu} dy_2^{\nu} + \dots \right) e^{\oint_{\mathcal{C}} i A_{\mu} dy^{\mu}} \right] \right\rangle \end{aligned} \quad (3.5)$$

To proceed, we use the Stokes theorem to the first term and write

$$\oint_{\delta\mathcal{C}_x} i A_{\mu} dy^{\mu} = \frac{i (\partial_{\mu} A_{\nu}(x) - \partial_{\nu} A_{\mu}(x))}{2} \delta \sigma^{\mu\nu}. \quad (3.6)$$

For the second term, we split it into the symmetric and the antisymmetric parts

$$\begin{aligned} &- \text{P} \left(\frac{1}{2} \oint_{\delta\mathcal{C}_x \times \delta\mathcal{C}_x} A_{\mu}(y_1) A_{\nu}(y_2) dy_1^{\mu} dy_2^{\nu} \right) = \\ &\underbrace{- \frac{1}{2} \left(\oint_{\delta\mathcal{C}_x} A_{\mu}(x) dx^{\mu} \right)^2}_{\text{Sym}} - \underbrace{\frac{1}{2} \oint_{\substack{\delta\mathcal{C}_x \times \delta\mathcal{C}_x \\ y_1 > y_2}} [A_{\mu}(y_1), A_{\nu}(y_2)] dy_1^{\mu} dy_2^{\nu}}_{\text{Asym}}. \end{aligned} \quad (3.7)$$

Here $y_1 > y_2$ means that the integral is path-ordered and y_2 is always behind y_1 . Since $\delta\mathcal{C}_x$ is an infinitesimal contour around x , the antisymmetric part can be approximated as

$$\begin{aligned}\text{Asym} &\simeq -\frac{[A_\mu(x), A_\nu(x)]}{2} \oint_{\substack{\delta\mathcal{C}_x \times \delta\mathcal{C}_x \\ y_1 > y_2}} dy_1^\mu dy_2^\nu \\ &= \frac{[A_\mu(y), A_\nu(y)]}{2} \oint_{\delta\mathcal{C}_x} y_2^\mu dy_2^\nu = \frac{[A_\mu(x), A_\nu(x)]}{2} \delta\sigma^{\mu\nu}.\end{aligned}\tag{3.8}$$

The sum of (3.6) and (3.8) gives $iF_{\mu\nu}(y)/2$ with $F_{\mu\nu} = \partial_\mu A_\nu - \partial_\nu A_\mu - i[A_\mu, A_\nu]$.

On the other hand, the symmetric part at one loop reads (see figure 6)

$$\langle \text{Sym} \rangle|_{1\text{-loop}} = -\frac{N}{2} \oint_{\delta\mathcal{C}_x} dy_1^\mu \oint_{\delta\mathcal{C}_x} dy_2^\nu G_{\mu\nu}(y_1 - y_2) \times \mathbf{1}\tag{3.9}$$

Here $\mathbf{1}$ is the identity matrix for the color factors and $G_{\mu\nu}(x_1 - x_2)$ is a propagator of gauge fields without color factors. In the axial gauge ($A_1 = 0$), it reads⁴

$$G_{\mu\nu}(x - y) = -\delta_\mu^2 \delta_\nu^2 \frac{g_{2d}^2}{4} \delta(x^2 - y^2) |x^1 - y^1|.\tag{3.10}$$

Plugging this into (3.9), we get

$$\langle \text{Sym} \rangle|_{1\text{-loop}} = -\frac{g_{2d}^2 N}{4} |\delta\sigma|.\tag{3.11}$$

A couple of comments are in order: First, the result (3.9) receives higher loop corrections. However since g_{2d} has mass dimension 1, it follows from dimensional analysis that the loop corrections come with higher powers of $\delta\sigma^{\mu\nu}$ and therefore can be neglected in the small area limit $\delta\sigma^{\mu\nu} \rightarrow 0$. Second, although (3.11) was computed in a specific gauge, the result is actually gauge-invariant. This is because the tree-level⁵ gauge transformation

$$A_\mu(y) \mapsto A_\mu(y) + \partial_\mu \alpha(y),\tag{3.12}$$

only changes (3.9) by a term that integrates to zero:

$$\delta\text{Sym} \propto \oint_{\delta\mathcal{C}_x} dy_1^\mu \partial_\mu \alpha(y_1) \oint_{\delta\mathcal{C}_x} dy_2^\nu \partial_\nu \alpha(y_2) = 0.\tag{3.13}$$

Third, the result (3.9) is for the $U(N)$ gauge group and the answer will be different for other gauge groups. It would be interesting to derive the loop equation for general gauge groups.

Now, combining the symmetric and antisymmetric parts, we arrive at the following expression for the first-order variation:

$$\frac{\delta\langle \tilde{\mathcal{W}}_{\mathcal{C}} \rangle}{\delta\sigma^{\mu\nu}(x)} = \left\langle \text{trP} \left[iF_{\mu\nu}(x) e^{\oint_{\mathcal{C}} iA_\mu dy^\mu} \right] \right\rangle - \frac{g_{2d}^2 N}{4} n_{\mu\nu}(x) \langle \tilde{\mathcal{W}}_{\mathcal{C}} \rangle.\tag{3.14}$$

⁴Note that our normalization for the coupling constant in 2d YM is different from [5]: $(g_{2d}^{[5]})^2 = (g_{2d}^{\text{ours}})^2/2$.

⁵As stated above, the higher-loop corrections can be neglected in the small area limit.

Let us make some clarification on the second term in (3.14): First, it contains the orientation tensor $n_{\mu\nu}$ and changes discontinuously across the contour. This property plays a crucial role in the derivation below. Second, it may appear to contradict a familiar statement that the small deformation of the Wilson loop is simply given by the insertion of $F_{\mu\nu}$. This apparent contradiction comes from the difference of the regularizations: Normally we insert $F_{\mu\nu}$ on top of the Wilson loop and regularize divergent diagrams which contract $F_{\mu\nu}$ and the loop by the principal value prescription. On the other hand, $F_{\mu\nu}$ in (3.14) is inserted slightly above or below the loop, which gives a different regularization. This alternative regularization produces a different answer, but one can show by the explicit computation⁶ that the sum of the two terms in (3.14) reproduces the result in the principal value prescription. We thus have

$$\frac{\delta\langle\tilde{\mathcal{W}}_C\rangle}{\delta\sigma^{\mu\nu}(x)} = \left\langle \text{trP} \left[iF_{\mu\nu}(x) e^{\oint_C iA_\mu dy^\mu} \right] \right\rangle \Big|_{\text{principal value}}, \quad (3.16)$$

which is consistent with the familiar statement.

Now we derive the loop equation. First we differentiate (3.14) and get

$$\partial^\mu \frac{\delta\langle\tilde{\mathcal{W}}_C\rangle}{\delta\sigma^{\mu\nu}(x)} = \left\langle \text{trP} \left[i\nabla^\mu F_{\mu\nu}(x) e^{\oint_C iA_\mu dy^\mu} \right] \right\rangle - \frac{g_{2d}^2 N}{4} \partial^\mu n_{\mu\nu}(x) \langle\tilde{\mathcal{W}}_C\rangle. \quad (3.17)$$

To evaluate $\partial^\mu n_{\mu\nu}$ that appears in the second term, it is useful to go back to the definition

$$\partial^\mu \frac{\delta\langle\tilde{\mathcal{W}}_C\rangle}{\delta\sigma^{\mu\nu}(x)} := \lim_{\varepsilon \rightarrow 0} \frac{1}{\varepsilon} \left(\frac{\delta\langle\tilde{\mathcal{W}}_C\rangle}{\delta\sigma^{\mu\nu}(x + \epsilon_\mu/2)} - \frac{\delta\langle\tilde{\mathcal{W}}_C\rangle}{\delta\sigma^{\mu\nu}(x - \epsilon_\mu/2)} \right). \quad (3.18)$$

Here we take x to be a point on the Wilson loop and ϵ_μ to be a vector of length ε in the μ direction; $(\epsilon_\mu)^\rho := \varepsilon \delta_\mu^\rho$. Since the points $x \pm \epsilon_\mu/2$ sit on different sides of the loop, we have $n_{\mu\nu}(x \pm \epsilon_\mu/2) = \pm 1$. Thus the derivative $\partial^\mu n_{\mu\nu}$ picks up a contribution from a delta function

$$\partial^\mu n_{\mu\nu}(x) = 2 \int_{I_x} dx'_\nu \delta^{(2)}(x' - x), \quad (3.19)$$

where the contour I_x is an infinitesimal one-dimensional segment which passes through x . Second we use the fact that $\nabla^\mu F_{\mu\nu}$ is proportional to the equation of motion⁷

$$\nabla^\mu F_{\mu\nu} = -\frac{g_{2d}^2}{2} \frac{\delta S_{2d}}{\delta A^\nu}. \quad (3.20)$$

We can then replace it inside the expectation value as

$$\left\langle (\nabla^\mu F_{\mu\nu}(x))^a{}_b \cdots \right\rangle \mapsto -\frac{g_{2d}^2}{2} \left\langle \frac{\delta}{\delta (A^\nu(x))^b{}_a} (\cdots) \right\rangle. \quad (3.21)$$

⁶In the holomorphic gauge $A_{\bar{z}} = 0$, the contraction of $F_{\mu\nu}$ and the straight-line loop reads (see e.g. [22])

$$\int_{-\infty}^{\infty} dy \langle i * F_{z\bar{z}}(x) i A_z(y) \rangle = -\frac{g_{2d}^2 N}{4\pi} \int_{-\infty}^{\infty} dy \frac{i}{1+y^2} \frac{1+xy}{x-y}. \quad (3.15)$$

In the principal value prescription, this integral vanishes while if we shift x slightly above or below by adding $\pm i\epsilon$, it gives $\pm g_{2d}^2 N/(4\pi)$, which are precisely canceled by the second term in (3.14).

⁷ S_{2d} is the Euclidean action for 2d YM given by (2.4).

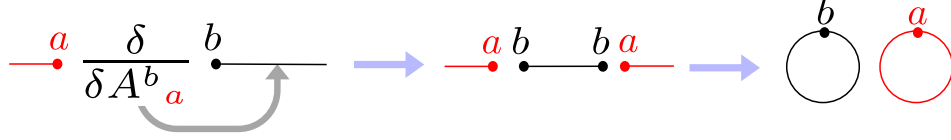


Figure 7: The Ward identity on the Wilson loop. The insertion of $\nabla^\mu F_{\mu\nu}$ on the loop can be replaced with the functional derivative $\delta/\delta A_\nu$. When it acts on other parts of the contour, it cuts the loop and reconnects it as shown in the figure.

Here we wrote the gauge indices a and b explicitly for convenience. As a result we get (see also figure 7)

$$\begin{aligned} \left\langle \text{trP} \left[i \nabla^\mu F_{\mu\nu}(x) e^{\oint_C i A_\mu dy^\mu} \right] \right\rangle &= -i \frac{g_{2d}^2}{2} \left\langle \frac{\delta}{\delta (A^\nu(x))^b_a} \left[\text{P} e^{\oint_C i A_\mu dy^\mu} \right]^b_a \right\rangle \\ &= \frac{g_{2d}^2}{2} \oint_C dx'_\nu \delta^{(2)}(x' - x) \left\langle \text{trP} \left[e^{\oint_{x'} i A_\mu dy^\mu} \right] \text{trP} \left[e^{\oint_C i A_\mu dy^\mu} \right] \right\rangle. \end{aligned} \quad (3.22)$$

The integral (3.22) is nonzero even for nonintersecting Wilson loops since it receives a contribution from a “self contraction”, namely a contribution from a trivial coincidence point $x' = x$ on the loop. It can be evaluated as

$$\begin{aligned} (\text{self-contraction}) &= \frac{g_{2d}^2}{2} \int_{I_x} dx'_\nu \delta^{(2)}(x' - x) \left\langle \text{trP} \left[e^{\oint_C i A_\mu dy^\mu} \right] \text{tr} [\mathbf{1}] \right\rangle \\ &= \frac{g_{2d}^2 N}{2} \int_{I_x} dx'_\nu \delta^{(2)}(x' - x) \left\langle \text{trP} \left[e^{\oint_C i A_\mu dy^\mu} \right] \right\rangle. \end{aligned} \quad (3.23)$$

As can be seen from (3.19), this turns out to cancel the second term in (3.17). Thus, when the two terms in (3.17) are combined, we are left with contributions only from intersecting points and obtain the loop equation

$$\partial^\mu \frac{\delta \langle \tilde{W}_C \rangle}{\delta \sigma^{\mu\nu}(x)} = \frac{g_{2d}^2}{2} \oint_C dx'_\nu \delta^{(2)}(x' - x) \left\langle \text{trP} \left[e^{\oint_{x'} i A_\mu dy^\mu} \right] \text{trP} \left[e^{\oint_C i A_\mu dy^\mu} \right] \right\rangle, \quad (3.24)$$

where the symbol \oint_C means that we remove an infinitesimal segment around x when we perform the integral. For the actual application, it is useful to choose ν to be the direction of the Wilson loop near the intersection and μ to be the direction orthogonal to it. In addition, we integrate (3.24) along a small path in the μ direction. For the left hand side, this is basically equivalent to going back to the definition (3.18) and removing $1/\varepsilon$, which

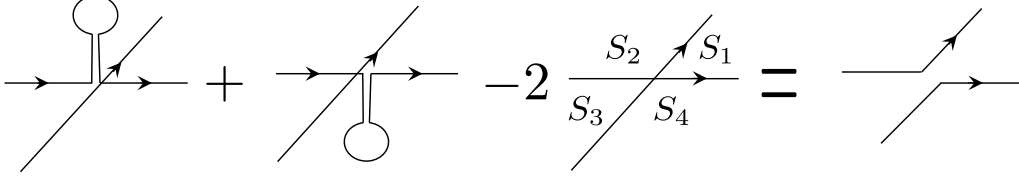


Figure 8: The area derivatives and the loop laplacian \hat{L}_x . The left hand side is the definition of \hat{L}_x which can be easily translated into area derivatives. (Adapted from [5].)

can be pictorially represented as⁸

$$\begin{aligned}
\hat{L}_x \langle \tilde{\mathcal{W}}_C \rangle &:= \lim_{\varepsilon \rightarrow 0} \frac{\delta \langle \tilde{\mathcal{W}}_C \rangle}{\delta \sigma^{\mu\nu}(x + \epsilon_\mu/2)} - \frac{\delta \langle \tilde{\mathcal{W}}_C \rangle}{\delta \sigma^{\mu\nu}(x - \epsilon_\mu/2)} \\
&= \frac{1}{\delta \sigma^{\mu\nu}(x + \frac{\epsilon_\mu}{2})} \left(\text{diagram with loop on top at } x + \frac{\epsilon}{2} - \text{diagram with loop on bottom at } x - \frac{\epsilon}{2} \right) \\
&= \frac{1}{|\delta \sigma|} \left(\text{diagram with loop on top at } x + \frac{\epsilon}{2} + \text{diagram with loop on bottom at } x - \frac{\epsilon}{2} - 2 \text{diagram with two parallel lines} \right). \tag{3.25}
\end{aligned}$$

We then get

$$\hat{L}_x \langle \tilde{\mathcal{W}}_C \rangle = \frac{g_{2d}^2}{2} \langle \tilde{\mathcal{W}}_{C_1} \tilde{\mathcal{W}}_{C_2} \rangle, \tag{3.26}$$

where $\mathcal{C}_{1,2}$ are the two contours obtained by reconnecting the loop \mathcal{C} at the point x . Here we assumed that only two lines intersect at the point x . When more than two lines intersect, the right hand side of (3.26) is replaced by a sum of all possible reconnections.

Using the fact that the Wilson loops in 2d YM only depend on the area, we can convert (3.26) to area derivatives (see figure 8),

$$\hat{L}_x \langle \tilde{\mathcal{W}}_C \rangle = (\partial_{S_1} + \partial_{S_3} - \partial_{S_2} - \partial_{S_4}) \langle \tilde{\mathcal{W}}_C \rangle = \frac{g_{2d}^2}{2} \langle \tilde{\mathcal{W}}_{C_1} \tilde{\mathcal{W}}_{C_2} \rangle. \tag{3.27}$$

This formula can be applied straightforwardly when the loop is on R^2 . For loops on S^2 , not all the areas (S_i 's) are independent. In such a case, we go back to the pictorial definition of \hat{L}_x given in (3.25) and translate it into area derivatives as we see in the next subsection.

3.2 Intersecting BPS loops in $\mathcal{N} = 4$ SYM

We now apply the loop equation (3.27) and compute the expectation value of intersecting 1/8-BPS loops in $\mathcal{N} = 4$ SYM.

⁸In the last equality, we used $\delta \sigma^{\mu\nu}(x + \epsilon_\mu/2) = -\delta \sigma^{\mu\nu}(x - \epsilon_\mu/2) = |\delta \sigma|$.

3.2.1 Figure eight loop

The simplest intersecting loop is the “figure eight” loop. Since the figure eight loop on S^2 is equivalent to a one-intersection loop (see figure 9), we start with the latter, and the result for the figure-eight can be simply obtained by relating the areas as in figure 9.

Under the action of \hat{L}_x , the one-intersection loop $\tilde{\mathcal{W}}_{A_1, A_2}$ reconnects to a product of two disconnected loops $\mathcal{W}_{1,2}$ with areas $A_{1,2}$. Using (3.25), this can be translated into area derivatives as follows⁹:

$$(\partial_{A_1} - \partial_{A_2})\langle \tilde{\mathcal{W}}_{A_1, A_2} \rangle = -\frac{4\pi g^2}{N}\langle \tilde{\mathcal{W}}_1 \tilde{\mathcal{W}}_2 \rangle. \quad (3.28)$$

Here we rewrote g_{2d} in terms of the coupling in $\mathcal{N} = 4$ SYM using (2.3) and (2.16): $g_{2d}^2 = -g_{YM}^2/(2\pi) = -8\pi g^2/N$. Dividing both sides by N , we get the equation for the normalised expectation value

$$(\partial_{A_1} - \partial_{A_2})\langle \mathcal{W}_{A_1, A_2} \rangle = -4\pi g\langle \mathcal{W}_1 \mathcal{W}_2 \rangle. \quad (3.29)$$

This can be solved by replacing the right hand side with the integrals (2.42). The result reads

$$\langle \mathcal{W}_{A_1, A_2} \rangle = \left\langle 4\pi g^2 i \oint \frac{du_1}{8\pi^2 g^2} \frac{du_2}{8\pi^2 g^2} \bar{\Delta}(u_1, u_2) \frac{f_{A_1}(u_1) f_{A_2}(u_2)}{u_1 - u_2} + \frac{1}{2} \oint \frac{du}{8\pi^2 g^2} f_{A_1}(u) f_{A_2}(u - i\epsilon) \right\rangle_M. \quad (3.30)$$

Alternatively, one can use (2.46) to write

$$\langle \mathcal{W}_{A_1, A_2} \rangle = \left\langle 4\pi g^2 i \oint_{\mathcal{C}_1 \prec \mathcal{C}_2} \frac{du_1}{8\pi^2 g^2} \frac{du_2}{8\pi^2 g^2} \bar{\Delta}(u_1, u_2) \frac{f_{A_1}(u_1) f_{A_2}(u_2)}{u_1 - u_2} \right\rangle_M. \quad (3.31)$$

Translating this to the figure eight loop using the relation (see figure 9),

$$A_1 = 4\pi - \bar{A}_1 \quad A_2 = \bar{A}_2, \quad (3.32)$$

we obtain (1.1) in the introduction. A simple consistency check of (3.30) is to consider the special case $A_2 = A_1$, which yields a doubly-wound fundamental Wilson loop. For $A_2 = A_1$, the double-integral in (3.30) vanishes due to antisymmetry of the integrand, and the single integral reproduces the expected result for the doubly-wound loop, which is given by (2.26) with $g_{YM} \rightarrow 2g_{YM}$.¹⁰

⁹To derive this, one simply needs to note that the first term (3.25) decreases A_2 while the second term increases A_1 when applied to the one-intersection loop.

¹⁰For a k -wound fundamental loop, it is easy to see from the Gaussian matrix model (2.5) that

$$\langle W_{k\text{-wound}} \rangle = \langle W_{\text{single}} \rangle|_{g_{YM} \rightarrow k g_{YM}}.$$

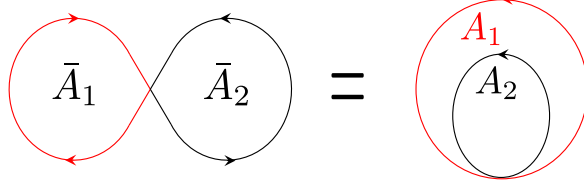


Figure 9: The figure eight loop and the one-intersection loop. On S^2 , one can continuously deform one to the other. In the right figure, the areas of the outer and inner circles are denoted by $A_{1,2}$ respectively. The areas are related by $A_1 = 4\pi - \bar{A}_1$ and $A_2 = \bar{A}_2$.

Large N In the large N limit, one can evaluate the integral (3.31) explicitly. To do so, we first replace the expectation values of f_A 's with their large N results,

$$\left\langle \prod_k f_{A_k}(u_k) \right\rangle_M = \left\langle \prod_k e^{iA_k(u_k - \frac{i\epsilon}{2})} \frac{\det(u_k - M - i\epsilon)}{\det(u_k - M)} \right\rangle_M \stackrel{N \rightarrow \infty}{=} \prod_k \mathfrak{f}_{A_k}(u_k), \quad (3.33)$$

where \mathfrak{f}_A is given by

$$\mathfrak{f}_A(u) := e^{iAu - 4\pi i g^2 G(u)}, \quad (3.34)$$

and $G(u)$ is the large N resolvent

$$G(u) := \lim_{N \rightarrow \infty} \frac{1}{N} \left\langle \text{tr} \left(\frac{1}{u - M} \right) \right\rangle_M = \frac{1}{2g^2} \left(u - \sqrt{u^2 - 4g^2} \right). \quad (3.35)$$

We then get

$$\langle \mathcal{W}_{A_1, A_2} \rangle \stackrel{N \rightarrow \infty}{=} 4\pi g^2 i \oint_{\mathcal{C}_1 < \mathcal{C}_2} \frac{du_1}{8\pi^2 g^2} \frac{du_2}{8\pi^2 g^2} \frac{\mathfrak{f}_{A_1}(u_1) \mathfrak{f}_{A_2}(u_2)}{u_1 - u_2}. \quad (3.36)$$

Here we replaced $\bar{\Delta}/(u_1 - u_2)$ with its large N limit, $1/(u_1 - u_2)$. This coincides with the expression obtained in [8] for the figure eight loop at large N (after the redefinition of the areas (3.32)). Below we evaluate this integral explicitly in terms of the Bessel functions.

To proceed, we introduce the Zhukowski variable¹¹

$$u = -ig \left(x - \frac{1}{x} \right), \quad (3.37)$$

and express \mathfrak{f}_A as

$$\mathfrak{f}_A(x) = e^{2g\pi(x+1/x)} e^{2ga(x-1/x)}, \quad a := \frac{A - 2\pi}{2}. \quad (3.38)$$

Substituting this into (3.36), we get

$$\langle \mathcal{W}_{A_1, A_2} \rangle \stackrel{N \rightarrow \infty}{=} -\frac{1}{4\pi g} \oint_{\mathcal{C}_1 < \mathcal{C}_2} \frac{dx_1(x_1 + x_1^{-1})}{2\pi i x_1} \frac{dx_2(x_2 + x_2^{-1})}{2\pi i x_2} \frac{\mathfrak{f}_{A_1}(x_1) \mathfrak{f}_{A_2}(x_2)}{(x_1 - x_2)(1 + 1/x_1 x_2)}. \quad (3.39)$$

¹¹As shown in [25, 41], the expressions obtained from localization often coincide with the ones from integrability when expressed in terms of x . This suggests that our integration variable u is related to the rapidity of magnons, defined by $u_{\text{rapidity}} = g(x + 1/x)$, by $u_{\text{rapidity}} = \sqrt{4g^2 - u^2}$.

We then expand $1/(x_1 - x_2)(1 + 1/x_1 x_2)$, close the contour \mathcal{C}_1 at the origin, and then close the contour \mathcal{C}_2 at infinity using the formula [25, 42]

$$\rho_a^k I_k(4\pi g_a) = \int \frac{dx}{2\pi i x^{k+1}} e^{2\pi g(x+1/x)} e^{2ga(x-1/x)}, \quad (3.40)$$

with

$$g_a := g \sqrt{1 - \frac{a^2}{\pi^2}}, \quad \rho_a := \sqrt{\frac{\pi + a}{\pi - a}}. \quad (3.41)$$

As a result, we arrive at the following expression for the one-intersection loop,

$$\langle \mathcal{W}_{A_1, A_2} \rangle \stackrel{N \rightarrow \infty}{=} \frac{\mathcal{I}_0^{a_1} \mathcal{I}_1^{a_2}}{2\pi g_{a_2}} + \sum_{k=1}^{\infty} \frac{\rho_{a_1}^{-k} \mathcal{I}_k^{a_1}}{4\pi g} \left[\left(\rho_{a_2}^{k+1} + \frac{(-1)^k}{\rho_{a_2}^{k+1}} \right) \mathcal{I}_{k+1}^{a_2} + \left(\rho_{a_2}^{k-1} + \frac{(-1)^k}{\rho_{a_2}^{k-1}} \right) \mathcal{I}_{k-1}^{a_2} \right], \quad (3.42)$$

where we used a shorthand notation

$$\mathcal{I}_k^a := I_k(4\pi g_a). \quad (3.43)$$

Using the relation (3.32), one can translate this to the result for the figure-eight loop,

$$\langle \mathcal{W}_{\text{figure-eight}} \rangle \stackrel{N \rightarrow \infty}{=} \frac{\mathcal{I}_0^{\bar{a}_1} \mathcal{I}_1^{\bar{a}_2}}{2\pi g_{\bar{a}_2}} + \sum_{k=1}^{\infty} \frac{\rho_{\bar{a}_1}^k \mathcal{I}_k^{\bar{a}_1}}{4\pi g} \left[\left(\rho_{\bar{a}_2}^{k+1} + \frac{(-1)^k}{\rho_{\bar{a}_2}^{k+1}} \right) \mathcal{I}_{k+1}^{\bar{a}_2} + \left(\rho_{\bar{a}_2}^{k-1} + \frac{(-1)^k}{\rho_{\bar{a}_2}^{k-1}} \right) \mathcal{I}_{k-1}^{\bar{a}_2} \right]. \quad (3.44)$$

Two remarks are in order. First, the expression (3.44) is not manifestly symmetric under $\bar{A}_1 \leftrightarrow \bar{A}_2$. One can bring it into a symmetric form using the identities for the infinite sum of the Bessel functions. See Appendix A. Second, the infinite sum in (3.44) is convergent at finite coupling owing to the large k behavior of $I_k(z)$

$$I_k(z) \stackrel{k \rightarrow \infty}{\sim} \frac{(z/2)^k}{k!}, \quad z \text{ fixed}. \quad (3.45)$$

However, there is a subtlety in the strong-coupling expansion: The asymptotic expansion of the modified Bessel function reads

$$I_k(z) = \frac{e^z}{\sqrt{2\pi x}} \left(1 + \frac{1 - 4k^2}{8z} + \frac{9 - 40k^2 + 16k^4}{128x^2} + \dots \right), \quad (3.46)$$

and it gives a polynomial in k at each order. This leads to a divergence of the infinite sum when $\rho_{\bar{a}_1} > \rho_{\bar{a}_2}$ (i.e. $\bar{A}_1 > \bar{A}_2$). A more reliable approach at strong coupling is to perform the saddle-point analysis to the integral (3.39) as we see below.

Weak coupling expansion Here we present the weak-coupling expansion (up to two loops) of the figure eight loop obtained from (3.44):

$$\begin{aligned} \langle \mathcal{W}_{\text{figure-eight}} \rangle &\stackrel{N \rightarrow \infty}{=} 1 + \frac{g^2}{2} [-(\bar{A}_1 - \bar{A}_2)^2 + 4\pi(\bar{A}_1 + \bar{A}_2)] \\ &+ \frac{g^4}{12} [(\bar{A}_1 - \bar{A}_2)^4 - 8\pi(\bar{A}_1^3 + \bar{A}_2^3) + 16\pi^2(\bar{A}_1^2 + 4\bar{A}_1\bar{A}_2 + \bar{A}_2^2)] + O(g^6), \end{aligned} \quad (3.47)$$

As expected, the result is symmetric under the exchange $\bar{A}_1 \leftrightarrow \bar{A}_2$ and reduces to the one for a single Wilson loop when $\bar{A}_2 = 0$. The result for the one-intersection loop can be obtained by the replacement $\bar{A}_1 = 4\pi - A_1$ and $\bar{A}_2 = A_2$.

Strong coupling expansion To perform the strong coupling expansion of the figure eight loop, we do the saddle point analysis to the integral (3.36) with the replacement (3.32). For definiteness, we assume¹² $\bar{A}_1 < \bar{A}_2$ below.

The saddle points are determined purely by the exponent of f_A 's and we find two saddle points for each variable

$$x_1 = \pm \rho_{\bar{a}_1}, \quad x_2 = \pm 1/\rho_{\bar{a}_2}. \quad (3.48)$$

Owing to the geometrical constraint $\bar{A}_1 + \bar{A}_2 \leq 4\pi$ and the assumption $\bar{A}_1 < \bar{A}_2$, we have $|\rho_{\bar{a}_1}| < |1/\rho_{\bar{a}_2}|$. Thus, the saddle points can be reached by deforming the original contours $\mathcal{C}_1 \prec \mathcal{C}_2$ without making the contours pass through¹³ each other. Among those four saddle points, the ones with plus signs are always dominant. Expanding the integral around the saddle point using the coordinates $x_1 = it_1 + \rho_{\bar{a}_1}$ and $x_2 = it_2 + 1/\rho_{\bar{a}_2}$, we get

$$\begin{aligned} \langle \mathcal{W}_{\text{figure-eight}} \rangle &\stackrel{N \rightarrow \infty}{=} \underbrace{\frac{-e^{4\pi(g_{\bar{a}_1} + g_{\bar{a}_2})}}{4\pi g(\pi + \bar{a}_1)(\pi - \bar{a}_2)(\rho_{\bar{a}_1} - \frac{1}{\rho_{\bar{a}_2}})(1 + \frac{\rho_{\bar{a}_1}}{\rho_{\bar{a}_2}})}}_{\text{saddle}} \underbrace{\int dt_1 e^{-\frac{2\pi g_{\bar{a}_1}}{\rho_{\bar{a}_1}^2} t_1^2} \int dt_2 e^{-2\pi g_{\bar{a}_2} \rho_{\bar{a}_2}^2 t_2^2}}_{\text{1-loop}} \\ &= -\frac{e^{4\pi(g_{\bar{a}_1} + g_{\bar{a}_2})}}{16\pi^2(g_{\bar{a}_1}\bar{a}_2 + g_{\bar{a}_2}\bar{a}_1)\sqrt{g_{\bar{a}_1}g_{\bar{a}_2}}} + \dots \end{aligned} \quad (3.49)$$

Performing similar analysis to other saddle points, we get a sum

$$\begin{aligned} \langle \mathcal{W}_{\text{figure-eight}} \rangle &\stackrel{N \rightarrow \infty}{=} \\ &\frac{-1}{16\pi^2\sqrt{g_{\bar{a}_1}g_{\bar{a}_2}}} \left[\frac{e^{4\pi(g_{\bar{a}_1} + g_{\bar{a}_2})} - e^{-4\pi(g_{\bar{a}_1} + g_{\bar{a}_2})}}{g_{\bar{a}_1}\bar{a}_2 + g_{\bar{a}_2}\bar{a}_1} - \frac{e^{4\pi(-g_{\bar{a}_1} + g_{\bar{a}_2})} - e^{4\pi(g_{\bar{a}_1} - g_{\bar{a}_2})}}{g_{\bar{a}_1}\bar{a}_2 - g_{\bar{a}_2}\bar{a}_1} \right]. \end{aligned} \quad (3.50)$$

To understand (3.50) from the string worldsheet, it is useful to recall the connected correlator of two Wilson loops $\langle \mathcal{W}_{A_1} \mathcal{W}_{A_2} \rangle$ analyzed in [17]. In that case, the BPS equation of the string worldsheet does not allow any connected surface and the only allowed surface is a degenerate cylinder made of two disks connected by a zero-area tube (see figure 10). Physically the zero-area tube corresponds to a propagator of a graviton and gives a factor of $1/N^2$. Combined with a factor g^2 which comes from integrating over the endpoints of the propagator, we obtain the correct g -dependence at strong coupling,

$$\langle \mathcal{W}_{A_1} \mathcal{W}_{A_2} \rangle \sim \underbrace{\frac{e^{4\pi g_{A_1}}}{g^{3/2}} \frac{e^{4\pi g_{A_2}}}{g^{3/2}}}_{\text{disconnected disks}} \times \underbrace{\frac{1}{N^2}}_{\text{propagator}} \times \underbrace{g^2}_{\text{endpoints}} = \frac{e^{4\pi(g_{A_1} + g_{A_2})}}{gN^2}. \quad (3.51)$$

¹²Since the result (3.44) is symmetric under the exchange of $\bar{A}_{1,2}$, the result for the other case $\bar{A}_1 \geq \bar{A}_2$ can be obtained by a simple replacement $\bar{A}_1 \leftrightarrow \bar{A}_2$.

¹³When the contours pass through each other, the saddle point approximation can potentially fail owing to the term $1/(x_1 - x_2)(1 + 1/x_1 x_2)$ in the integrand.

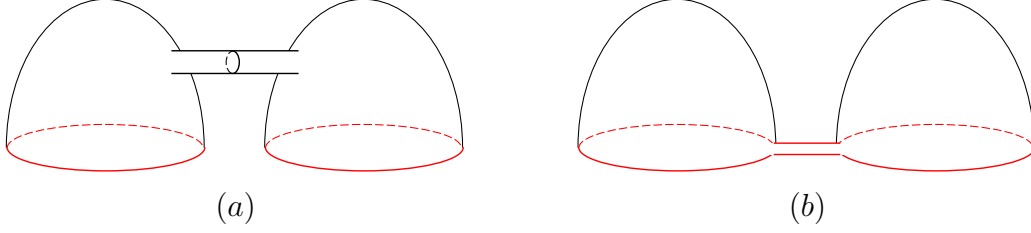


Figure 10: (a) The classical string configuration for the connected part of $\langle \mathcal{W}_{A_1} \mathcal{W}_{A_2} \rangle$. It consists of two disconnected surfaces joined together by an infinitesimal tube. (b) The classical string configuration for the figure eight loop. In this case, two disconnected surfaces are connected by an infinitesimal strip. This explains the difference of the prefactors in (3.51) and (3.52).

A similar argument seems to hold for (3.50): The idea is to consider a degenerate disk made of two disconnected worldsheet with disk topology (ending on the two loops of the figure-eight), joined together by a zero-area *strip* (see figure 10). The zero-area strip can be viewed as a propagator of an open string and gives a factor of $1/g$. Combined with other factors, it gives

$$\langle \mathcal{W}_{\text{figure-eight}} \rangle \sim \underbrace{\frac{e^{4\pi g \bar{a}_1}}{g^{3/2}} \frac{e^{4\pi g \bar{a}_2}}{g^{3/2}}}_{\text{disconnected disks}} \times \underbrace{\frac{1}{g}}_{\text{propagator}} \times \underbrace{g^2}_{\text{endpoints}} = \frac{e^{4\pi(g\bar{a}_1 + g\bar{a}_2)}}{g^2}, \quad (3.52)$$

which is the correct g -dependence in (3.50). The other three saddle points can be interpreted similarly as contributions from stable/unstable disk solutions [17, 43] joined by a zero-area strip. It would be interesting to perform more detailed analysis and reproduce the full one-loop answer including the numerical coefficients. (See [44, 45] for recent progress on the one-loop computation on the worldsheet for a single Wilson loop.)

3.2.2 Two-intersection loop

We now generalize the analysis to the two-intersection loop $\tilde{\mathcal{W}}_{A_1, A_2, A_3}$ depicted in figure 11. Applying the loop equation to the intersection shown in figure 12, we obtain

$$(\partial_{A_1} + \partial_{A_3}) \langle \tilde{\mathcal{W}}_{A_1, A_2, A_3} \rangle = -\frac{4\pi g^2}{N} \langle \tilde{\mathcal{W}}_{A_1, (A_2 - A_3)} \rangle, \quad (3.53)$$

where $\tilde{\mathcal{W}}_{A_1, (A_2 - A_3)}$ is a one-intersection loop with areas A_1 and $A_2 - A_3$. Solving this equation using (3.31) and normalizing it as¹⁴

$$\mathcal{W}_{A_1, A_2, A_3} := \frac{\tilde{\mathcal{W}}_{A_1, A_2, A_3}}{N^2}, \quad (3.54)$$

we get

$$\langle \mathcal{W}_{A_1, A_2, A_3} \rangle = F(A_1 - A_3, A_2) - \frac{(4\pi g^2)^2}{N^2} \left\langle \oint_{\mathcal{C}_1 \prec \mathcal{C}_2} \frac{du_1}{8\pi^2 g^2} \frac{du_2}{8\pi^2 g^2} \bar{\Delta} \frac{f_{A_1}(u_1) f_{A_2 - A_3}(u_2)}{(u_1 - u_2)^2} \right\rangle_M,$$

¹⁴The normalization is chosen such that the expectation value is $O(1)$ in the large N limit.

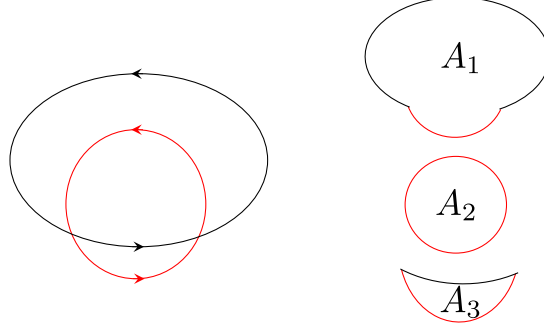


Figure 11: The two intersection loop and the definition of the areas. A_1 is the area of the whole regions inside the loop while A_2 is the area inside the red circle. A_3 is the area inside a small subregion in the bottom bounded by the red and black curves.

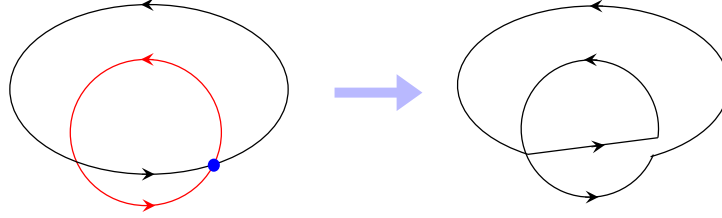


Figure 12: The action of the loop equation on the two intersection loop. After using the loop equation to the point colored in blue, we obtain a one-intersection loop with areas A_1 and $A_2 - A_3$.

where $F(A_1 - A_3, A_2)$ is the integration constant. To determine F , we consider the limit $A_3 \rightarrow 0$, in which the two-intersection Wilson loop reduces to two disconnected Wilson loops with areas A_1 and A_2 respectively. We then get the constraint

$$\langle \mathcal{W}_{A_1, A_2, A_3} \rangle|_{A_3=0} = \left\langle \oint_{C_1 \prec C_2} \frac{du_1}{8\pi^2 g^2} \frac{du_2}{8\pi^2 g^2} \bar{\Delta} f_{A_1}(u_1) f_{A_2}(u_2) \right\rangle_M, \quad (3.55)$$

which allows us to compute F . As a result, we get

$$\begin{aligned} \langle \mathcal{W}_{A_1, A_2, A_3} \rangle &= \left\langle \oint_{C_1 \prec C_2} \frac{du_1}{8\pi^2 g^2} \frac{du_2}{8\pi^2 g^2} \bar{\Delta} f_{A_1 - A_3}(u_1) f_{A_2}(u_2) \right\rangle_M \\ &+ \left(\frac{4\pi g^2}{N} \right)^2 \left\langle \oint_{C_1 \prec C_2} \frac{du_1}{8\pi^2 g^2} \frac{du_2}{8\pi^2 g^2} \bar{\Delta} \frac{f_{A_1 - A_3}(u_1) f_{A_2}(u_2) - f_{A_1}(u_1) f_{A_2 - A_3}(u_2)}{(u_1 - u_2)^2} \right\rangle_M. \end{aligned} \quad (3.56)$$

Large N Let us next discuss the large N expansion of (3.56). For later purposes, we compute it up to the first subleading order in $1/N$.

First we consider the first term of (3.56) (to be denoted by W_1). It coincides with the integral representation of the two disconnected Wilson loops with areas $A_1 - A_3$ and A_2 (see

(2.46)). Thus, using the result in the literature, we get the large N expansion

$$W_1 \stackrel{N \rightarrow \infty}{=} \frac{\mathcal{I}_1^{a_{13}} \mathcal{I}_1^{a_2}}{4\pi^2 g_{a_{13}} g_{a_2}} + \frac{\pi}{6N^2} \left[\frac{g_{a_2}^2 \mathcal{I}_1^{a_{13}} \mathcal{I}_2^{a_2}}{g_{a_{13}}} + \frac{g_{a_{13}}^2 \mathcal{I}_1^{a_2} \mathcal{I}_2^{a_{13}}}{g_{a_2}} \right] + \frac{1}{N^2} \sum_{k=1}^{\infty} k \left(\frac{\rho_{a_2}}{\rho_{a_{13}}} \right)^k \mathcal{I}_k^{a_{13}} \mathcal{I}_k^{a_2}, \quad (3.57)$$

with $a_{ij} := (A_i - A_j - 2\pi)/2$. Here the first two terms come from the disconnected part, which is a product of the expectation values of a single loop¹⁵ [14], while the last term is the connected part computed in [17].

The second line of (3.56) (to be denoted by W_2) can be evaluated in a manner similar to the figure eight loop: Namely we replace f_A and $\bar{\Delta}/(u_1 - u_2)^2$ with \mathfrak{f}_A and $1/(u_1 - u_2)^2$ respectively, rewrite it in terms of the Zhukowski variables and perform the integrals by closing the contour \mathcal{C}_1 at the origin and \mathcal{C}_2 at infinity. The result reads

$$W_2 \stackrel{N \rightarrow \infty}{=} \frac{1}{N^2} \sum_{k=1}^{\infty} k \left[\frac{\mathcal{I}_k^{a_1} \mathcal{I}_k^{a_{23}}}{\rho_{a_1}^k} \left(\rho_{a_{23}}^k - \frac{(-1)^k}{\rho_{a_{23}}^k} \right) - \frac{\mathcal{I}_k^{a_{13}} \mathcal{I}_k^{a_2}}{\rho_{a_{13}}^k} \left(\rho_{a_2}^k - \frac{(-1)^k}{\rho_{a_2}^k} \right) \right].$$

Adding the two contributions, we get the large N answer

$$\begin{aligned} \langle \mathcal{W}_{A_1, A_2, A_3} \rangle \stackrel{N \rightarrow \infty}{=} & \frac{\mathcal{I}_1^{a_{13}} \mathcal{I}_1^{a_2}}{4\pi^2 g_{a_{13}} g_{a_2}} + \frac{\pi}{6N^2} \left(\frac{g_{a_2}^2 \mathcal{I}_1^{a_{13}} \mathcal{I}_2^{a_2}}{g_{a_{13}}} + \frac{g_{a_{13}}^2 \mathcal{I}_1^{a_2} \mathcal{I}_2^{a_{13}}}{g_{a_2}} \right) \\ & + \frac{1}{N^2} \sum_{k=1}^{\infty} k \left[\frac{\mathcal{I}_k^{a_1} \mathcal{I}_k^{a_{23}}}{\rho_{a_1}^k} \left(\rho_{a_{23}}^k - \frac{(-1)^k}{\rho_{a_{23}}^k} \right) + (-1)^k \frac{\mathcal{I}_k^{a_{13}} \mathcal{I}_k^{a_2}}{(\rho_{a_{13}} \rho_{a_2})^k} \right]. \end{aligned} \quad (3.59)$$

Weak coupling expansion From (3.59), the weak coupling expansion can be obtained straightforwardly by expanding each term in powers of g^2 . The result up to one loop reads

$$\begin{aligned} \langle \mathcal{W}_{A_1, A_2, A_3} \rangle \stackrel{N \rightarrow \infty}{=} & \quad (3.60) \\ 1 + g^2 \left(\frac{4\pi(A_1 + A_2 - A_3) - A_1^2 - A_2^2 - A_3^2 + 2A_1 A_3}{2} + \frac{4\pi(A_2 - A_3) - A_2(A_1 - A_3)}{N^2} \right). \end{aligned}$$

One can check that the result reproduces the one for the two disconnected loops [14, 17] in the limit $A_3 \rightarrow 0$.

Strong coupling expansion We now evaluate the strong-coupling limit of (3.56). The first term, W_1 , is easy to evaluate since it coincides with the correlator of disconnected

¹⁵The expectation value of a single loop up to $O(1/N^2)$ is given by [14]

$$\langle \mathcal{W}_A \rangle = \frac{I_1(4\pi g_a)}{2\pi g_a} + \frac{\pi^2 g_a^2}{3N^2} I_2(4\pi g_a) + \dots \quad (3.58)$$

Wilson loops with areas $A_1 - A_3$ and A_2 . Using the result in the literature [14, 17], we get

$$\begin{aligned}
W_1 &\stackrel{N \rightarrow \infty}{=} W_{1,\text{disc}} + W_{1,\text{conn}} , \\
W_{1,\text{disc}} &= \frac{e^{4\pi(g_{a_{13}}+g_{a_2})}}{8\pi^2(g_{a_{13}}g_{a_2})^{3/2}} \left(1 + \frac{2(\pi g_{a_{13}})^3}{3N^2}\right) \left(1 + \frac{2(\pi g_{a_2})^3}{3N^2}\right) , \\
W_{1,\text{conn}} &= \frac{e^{4\pi(g_{a_{13}}+g_{a_2})}}{8\pi^2 N^2 \sqrt{g_{a_{13}}g_{a_2}}} \frac{\rho_{a_{13}}\rho_{a_2}}{(\rho_{a_{13}} - \rho_{a_2})^2} ,
\end{aligned} \tag{3.61}$$

where we kept only the leading exponential. $W_{1,\text{disc}}$ and $W_{1,\text{conn}}$ are the contributions from the disconnected part and the connected part respectively. The second term in (3.56), W_2 , can be evaluated by the saddle point analysis. The result reads

$$W_2 \stackrel{N \rightarrow \infty}{=} \frac{1}{8N^2} \left(\frac{\sqrt{g_{a_1}g_{a_{23}}}e^{4\pi(g_{a_1}+g_{a_{23}})}}{(g_{a_1}a_{23} + g_{a_{23}}a_1)^2} - \frac{\sqrt{g_{a_{13}}g_{a_2}}e^{4\pi(g_{a_{13}}+g_{a_2})}}{(g_{a_{13}}a_2 + g_{a_2}a_{13})^2} \right) . \tag{3.62}$$

Let us discuss the worldsheet interpretation. $W_{1,\text{disc}}$ is simply a product of the contributions from two disconnected surfaces whose worldsheet interpretation is already discussed in [14]. The rest ($W_{1,\text{disc}}$ and W_2) scales as $W_{1,\text{disc}}, W_2 \sim e^{4\pi g}/(gN^2)$, which coincides with (3.51). This shows that the relevant worldsheet configurations are again two disconnected surfaces connected by a zero-area tube. The only complication here is that there are two different disconnected surfaces ending on the Wilson loop, corresponding to two different exponentials in (3.62). The first one ends on the closed loops with areas A_1 and $A_2 - A_3$ while the second one ends on the closed loops with areas $A_1 - A_3$ and A_2 (see also figure 11). However owing to the geometrical constraint $A_1 > A_2 > A_3$, we have $g_{a_{13}} + g_{a_2} \geq g_{a_1} + g_{a_{23}}$. Thus the leading strong coupling answer is always given by $\sim e^{4\pi(g_{a_{13}}+g_{a_2})}$.

4 Cross Anomalous Dimension at Small Angle

We now apply the results in the previous sections to the computation of the *cross anomalous dimension*. The cross anomalous dimension is a quantity which governs the UV divergence associated to an intersection of two Wilson lines. In some respects, it is similar to the cusp anomalous dimension, which governs the UV divergence associated to a cusp of the Wilson line. However, one notable difference is that the cross anomalous dimension is a 2×2 matrix since the intersecting Wilson lines mix with the “touching” Wilson lines (depicted in figure 13-(a)) under the renormalization group flow.

Note that there is another cross anomalous dimension which governs the mixing of two different touching Wilson lines depicted in figure 13-(b). As we show in Appendix B, our formalism can be applied to this quantity as well.

4.1 Cross anomalous dimension in $\mathcal{N} = 4$ SYM

Definition and the relation to amplitudes The cross anomalous dimension matrix Γ_{cross} determines the renormalization group (RG) property of the Wilson lines with an in-

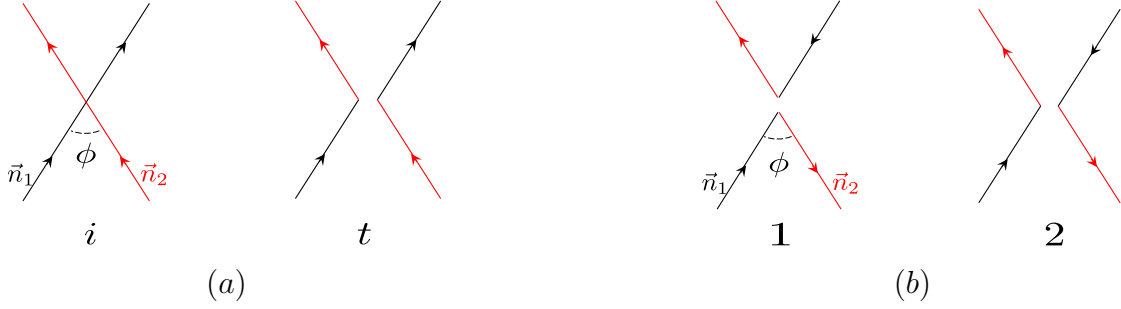


Figure 13: (a) Intersecting lines (denoted by i) and “touching” lines (denoted by t). They are characterized by a geometrical angle ϕ and mix under the renormalization. In $\mathcal{N} = 4$ SYM, we can consider the generalization of these lines which couple also to scalars. In that case, the black lines couple to $\vec{n}_1 \cdot \vec{\Phi}$ and the red lines couple to $\vec{n}_2 \cdot \vec{\Phi}$. This introduces an additional angle $\cos \theta = \vec{n}_1 \cdot \vec{n}_2$. (b) Two touching configurations (1 and 2) whose cross anomalous dimension will be computed in Appendix B.

tersection [27, 28]:

$$\left(\mu \frac{\partial}{\partial \mu} + \beta(g) \frac{\partial}{\partial g} \right) \mathcal{W}_A^R + (\Gamma_{\text{cross}})_A^B \mathcal{W}_B^R = 0 \quad (A, B = i, t), \quad (4.1)$$

Here μ is the RG scale and \mathcal{W}_i and \mathcal{W}_t denote the intersecting and the touching configurations respectively. The superscript R signifies the fact that the Wilson lines are renormalized and are related to the *bare* Wilson lines \mathcal{W}_A by the multiplicative renormalization,

$$\mathcal{W}_A^R = (Z(\mu, \epsilon))_A^B \mathcal{W}_B. \quad (4.2)$$

with ϵ being the UV cut-off. As we discuss in more detail later, in conformal field theories one can compute the cross anomalous dimension more directly from the expectation value of the bare Wilson lines by reading off the coefficient of $\log \epsilon$, $\langle \mathcal{W} \rangle \sim e^{\Gamma_{\text{cross}} \log \epsilon}$.

The cross anomalous dimension is a function of the angle ϕ between the two intersecting lines. When the angle is analytically continued as $\phi \rightarrow i\varphi$, it gives the so-called *soft anomalous dimension*. The soft anomalous dimension controls the IR divergence of the scattering amplitude of two massive quarks in the Regge kinematics, $s, m^2 \gg -t \gg \Lambda_{\text{QCD}}^2$, and describes how the soft gluons transfer the color degrees of freedom of the quarks. In that context, φ is the boost angle between the two quarks defined by

$$\cosh \varphi := -\frac{p_1 \cdot p_2}{\sqrt{p_1^2 p_2^2}}, \quad (4.3)$$

with $p_{1,2}$ being the four-momenta of the quarks. See [27, 28] for more details.

For the application to QCD, the limit $\varphi \rightarrow \infty$ is of particular interest since it describes the high energy scattering of light partons. On the Wilson line side, this corresponds to an intersection of two light-like lines, see for instance [46–48]. The limit was studied also in $\mathcal{N} = 4$ SYM: In [49], the self-crossing lightlike loop was analyzed up to nine loops. The analysis was pushed further in [50] in which the anomalous dimensions relevant for the limit

were determined exactly in the large N limit using the pentagon OPE decomposition [51]. In this paper, we focus on different limits, namely $\phi \sim \varphi \sim 0$ and the near BPS limit, and compute the anomalous dimension exactly at finite N .

Generalization in $\mathcal{N} = 4$ SYM In $\mathcal{N} = 4$ SYM, one can consider a generalization of the cross anomalous dimension $\Gamma_{\text{cross}}(\phi, \theta)$ which depends on another angle θ . To do so, we consider an intersection of the supersymmetric Wilson lines,

$$\mathcal{W} \sim \text{trP} \exp \left(\int (iA_\mu \dot{x}^\mu + \vec{n} \cdot \vec{\Phi} |\dot{x}|) d\tau \right), \quad (4.4)$$

where the *R-symmetry polarization* \vec{n} is a six-component unit vector which dictates the coupling to the scalars $\vec{\Phi} = (\Phi_1, \dots, \Phi_6)$. The intersection of such lines can be characterized by the geometric angle ϕ and the *R-symmetry angle* θ which is defined by

$$\cos \theta := \vec{n}_1 \cdot \vec{n}_2, \quad (4.5)$$

where $\vec{n}_{1,2}$ are the R-symmetry polarizations of the two lines at the intersection point.

The supersymmetric Wilson line (4.4) naturally arises from the worldline action of the W -boson in the Coulomb branch of $\mathcal{N} = 4$ SYM. To be concrete, let us consider the symmetry breaking phase $U(N+2) \rightarrow U(1) \times U(1) \times U(N)$ dictated by the scalar expectation value

$$\langle \vec{\Phi} \rangle = \text{diag} \left(m_1 \vec{n}_1, m_2 \vec{n}_2, \underbrace{0, \dots, 0}_N \right). \quad (4.6)$$

In this phase, we have two kinds of W -bosons, one coming from the $(1, k)$ (or $(k, 1)$) component and the other coming from the $(2, k)$ (or $(k, 2)$) component of the gauge field. In the limit $m_{1,2} \gg 1$, they can be treated as classical probe particles and their coupling to the unbroken $U(N)$ degrees of freedom is given precisely by (4.4). Thus $\Gamma_{\text{cross}}(\phi, \theta)$ gives a natural generalization of the cross anomalous dimension in QCD and it characterizes the IR divergence of the scattering of massive W -bosons after the analytic continuation $\phi \rightarrow i\varphi$.

When $\phi = \theta$, the whole configuration becomes BPS and the anomalous dimension $\Gamma_{\text{cross}}(\phi, \theta)$ vanishes. Expanding $\Gamma_{\text{cross}}(\phi, \theta)$ around this limit, we obtain¹⁶

$$\Gamma_{\text{cross}}(\phi, \theta) = (\phi - \theta) \gamma_{\text{cross}}(\theta) + O((\phi - \theta)^2). \quad (4.7)$$

In what follows, we compute the first coefficient $\gamma_{\text{cross}}(\theta)$ exactly as a function of λ and N .

4.2 Two-point function of intersections

Let us explain in more detail how to extract the cross anomalous dimension from the expectation values of the bare Wilson lines. The key idea is to regard them as the two-point functions of intersections.

¹⁶The relation between Γ_{cross} and $\hat{\gamma}_{\text{cross}}$ parallels the relation between the cusp anomalous dimension and the Bremsstrahlung function [24].

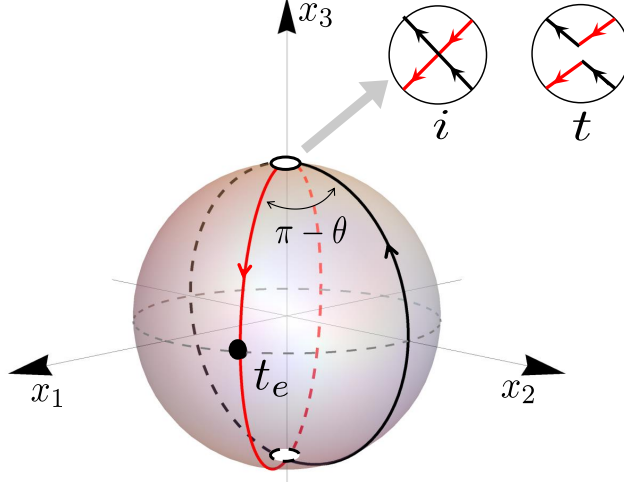


Figure 14: Intersecting lines mapped onto S^2 . The black and the red lines denote \mathcal{W}_1 and \mathcal{W}_2 respectively. On S^2 , the configuration contains two intersections, one at the north pole and the other at the south pole. At each intersection (denoted by white circles), one can make either of the two choices, i and t . This leads to the 2×2 matrix structure of the cross anomalous dimension.

To be concrete, consider the intersection of the following two Wilson lines on R^4 ,

$$\mathcal{W}_{1,2} = \text{P exp} \int_{-\infty}^{\infty} d\tau \left(iA \cdot \dot{x}_{1,2} + \vec{\Phi} \cdot \vec{n}_{1,2} |\dot{x}_{1,2}| \right), \quad (4.8)$$

with

$$\begin{aligned} \dot{x}_1 &= (1, 0, 0, 0), & \dot{x}_2 &= (\cos \phi, \sin \phi, 0, 0), \\ n_1 &= (1, 0, 0, 0, 0, 0), & n_2 &= (\cos \theta, \sin \theta, 0, 0, 0, 0). \end{aligned} \quad (4.9)$$

In addition to the obvious intersection at the origin, the lines intersect also at infinity. This is easier to see if one maps the configuration to S^2 using the conformal transformation

$$X_1 = \frac{2x_1}{1 + x_1^2 + x_2^2}, \quad X_2 = \frac{-2x_1}{1 + x_1^2 + x_2^2}, \quad X_3 = \frac{1 - x_1^2 - x_2^2}{1 + x_1^2 + x_2^2}. \quad (4.10)$$

Here X 's are the embedding coordinates of S^2 while x 's are the coordinates on R^2 inside R^4 . The two intersections are mapped to the north and the south poles of S^2 , see figure 14.

To extract the cross anomalous dimension, one has to consider the operator mixing: For each intersection, we can either let the lines intersect (to be denoted by i) or resolve the intersection and make the lines touching (to be denoted by t). Since there are two intersections, we have in total four different configurations of the Wilson lines which we denote by \mathcal{W}_{ii} , \mathcal{W}_{it} , \mathcal{W}_{ti} and \mathcal{W}_{tt} . They can be regarded as two-point functions of “operators”, labeled by i and t , sitting at the intersections.

These four choices of two-point functions can be naturally organized into a 2×2 matrix

$$\mathbb{W} := \begin{pmatrix} \langle \mathcal{W}_{ii} \rangle & \langle \mathcal{W}_{it} \rangle \\ \langle \mathcal{W}_{ti} \rangle & \langle \mathcal{W}_{tt} \rangle \end{pmatrix} = \begin{pmatrix} \langle i | \exp \left(D \log \frac{\epsilon_{UV}}{r_{IR}} \right) | i \rangle & \langle i | \exp \left(D \log \frac{\epsilon_{UV}}{r_{IR}} \right) | t \rangle \\ \langle t | \exp \left(D \log \frac{\epsilon_{UV}}{r_{IR}} \right) | i \rangle & \langle t | \exp \left(D \log \frac{\epsilon_{UV}}{r_{IR}} \right) | t \rangle \end{pmatrix}. \quad (4.11)$$

Here $\langle i, t |$ and $| i, t \rangle$ denote the intersections at the origin and infinity respectively and D is the dilatation operator. ϵ_{UV} and r_{IR} are the UV and the IR cutoffs. \mathbb{W} can be expressed alternatively in terms of the cross anomalous dimension Γ_{cross} and the overlap η as

$$\mathbb{W} = e^{\Gamma_{\text{cross}} \log(\epsilon_{\text{UV}}/r_{\text{IR}})} \cdot \eta, \quad (4.12)$$

where Γ_{cross} and η are 2×2 matrices defined by

$$\begin{pmatrix} \langle i |, & \langle t | \end{pmatrix} \Gamma_{\text{cross}} := \begin{pmatrix} \langle i | D, & \langle t | D \end{pmatrix}, \quad \eta := \begin{pmatrix} \langle i | i \rangle & \langle i | t \rangle \\ \langle t | i \rangle & \langle t | t \rangle \end{pmatrix}. \quad (4.13)$$

In the near BPS limit $\theta \sim \phi$, both η and Γ_{cross} can be expanded in powers of $(\phi - \theta)$,

$$\eta = \eta_0 + (\phi - \theta)\eta_1 + \dots, \quad \Gamma_{\text{cross}} = (\phi - \theta)\gamma_{\text{cross}} + \dots. \quad (4.14)$$

We then obtain the following expansion of the two-point function matrix \mathbb{W} :

$$\begin{aligned} \mathbb{W} &= \mathbb{W}_0 + (\phi - \theta)\mathbb{W}_1 + \dots, \\ \mathbb{W}_0 &= \eta_0, \quad \mathbb{W}_1 = \eta_1 + (\gamma_{\text{cross}} \cdot \eta_0) \log(\epsilon_{\text{UV}}/r_{\text{IR}}). \end{aligned} \quad (4.15)$$

Thus γ_{cross} is given by the coefficient of the logarithm in \mathbb{W}_1 , multiplied by $(\mathbb{W}_0)^{-1}$,

$$\gamma_{\text{cross}} = \left(\mathbb{W}_1 \Big|_{\log \frac{\epsilon_{\text{UV}}}{r_{\text{IR}}}} \right) \cdot (\mathbb{W}_0)^{-1}, \quad (4.16)$$

where \mathbb{W}_0 is nothing but the expectation value in the BPS limit:

$$\mathbb{W}_0(\theta) = \begin{pmatrix} \langle \mathcal{W}_{ii} \rangle & \langle \mathcal{W}_{it} \rangle \\ \langle \mathcal{W}_{ti} \rangle & \langle \mathcal{W}_{tt} \rangle \end{pmatrix} \Big|_{\phi=\theta}. \quad (4.17)$$

4.3 Cross anomalous dimension from localization

We now relate γ_{cross} given in (4.16) to the localization computation. This can be done by following the arguments in [22, 24, 25], which we briefly review below¹⁷.

The first step is to start with the BPS limit $\theta = \phi$ of (4.8) and deform θ slightly. This amounts to inserting a scalar on the second Wilson line

$$\delta \mathcal{W}_2 = \delta \theta \times \int_{-\infty}^{\infty} d\tau P[\Phi'(\tau) \mathcal{W}_2], \quad (4.18)$$

with

$$\Phi'(\tau) = -\sin \theta \Phi_1 + \cos \theta \Phi_2 \Big|_{x^\mu = (\tau \cos \theta, \tau \sin \theta, 0, 0, 0)}. \quad (4.19)$$

Now, using the invariance under the dilatation around the origin, we can determine the position dependence of the scalar insertion as

$$\langle \Phi'(\tau) \dots \rangle = \frac{1}{|\tau|} \langle \Phi'(\tau = 1) \dots \rangle, \quad (4.20)$$

¹⁷See section 4.2 of [25] for more detailed explanation.

where we denoted all the other parts (the Wilson lines $\mathcal{W}_{1,2}$ and possible resolutions of the intersections etc.) by \dots . From this, one can see that the integral of τ produces the logarithmic divergence and its coefficient is given by the expectation value of the Wilson loops with the Φ' insertion. More explicitly, we have the relation

$$\mathbb{W}_1|_{\log \frac{\epsilon_{UV}}{r_{IR}}} = 2 \left(\begin{array}{cc} \langle \mathcal{W}'_{ii} \rangle & \langle \mathcal{W}'_{it} \rangle \\ \langle \mathcal{W}'_{ti} \rangle & \langle \mathcal{W}'_{tt} \rangle \end{array} \right) \Big|_{\phi=\theta}, \quad (4.21)$$

where \mathcal{W}'_{AB} is the Wilson line \mathcal{W}_{AB} with Φ' inserted at $(\cos \theta, \sin \theta, 0, 0, 0, 0)$. The factor of 2 comes from summing up contributions from $\int_0^\infty d\tau$ and $\int_{-\infty}^0 d\tau$.

The second step is to map the whole configuration to S^2 using (4.10). We then get two great circles whose contour are given by

$$(x_1, x_2, x_3) = \begin{cases} (0, \sin t, -\cos t) & (\mathcal{W}_1) \\ (-\sin \theta \sin t, \cos \theta \sin t, -\cos t) & (\mathcal{W}_2) \end{cases}, \quad (4.22)$$

with $t \in (-\pi, \pi)$. They couple to Φ^1 and $\cos \theta \Phi^1 + \sin \theta \Phi^2$ respectively and satisfy the 1/8 BPS condition (2.1). Under this map, the insertion $\Phi'(\tau = 1)$ is mapped to the insertion at a point t_e where \mathcal{W}_2 intersects with the equator of S^2 (see figure 14).

The third step is to replace Φ' at t_e with $\Phi' - i\Phi_4 =: -\tilde{\Phi}$. This replacement does not affect the expectation values since the correlator with Φ_4 vanishes owing to the charge conservation. We then use the fact that the insertion of $\tilde{\Phi}$ corresponds to the insertion of the field strength in 2d YM [10, 15]. Therefore its expectation value can be computed by taking the area derivative. In our setup there are two regions with area $2(\pi - \theta)$, and changing θ by $\delta\theta$ leads to a total change (decrease) of the area by $4\delta\theta$. We thus have the relation

$$\left(\begin{array}{cc} \langle \mathcal{W}'_{ii} \rangle & \langle \mathcal{W}'_{it} \rangle \\ \langle \mathcal{W}'_{ti} \rangle & \langle \mathcal{W}'_{tt} \rangle \end{array} \right) \Big|_{\phi=\theta} = \frac{1}{4} \partial_\theta \mathbb{W}_0(\theta), \quad (4.23)$$

with \mathbb{W}_0 is the expectation value in the BPS limit (4.17). Combined with (4.21), it gives

$$\mathbb{W}_1|_{\log \frac{\epsilon_{UV}}{r_{IR}}} = \frac{1}{2} \partial_\theta \mathbb{W}_0(\theta). \quad (4.24)$$

Using (4.16), we get the formula relating γ_{cross} to the BPS Wilson loops

$$\gamma_{\text{cross}} = \frac{1}{2} (\partial_\theta \mathbb{W}_0) \cdot (\mathbb{W}_0)^{-1}. \quad (4.25)$$

Before we proceed, let us comment on the normalization. In what follows, we normalize \mathbb{W}_0 by dividing the path-ordered exponentials by a common factor N^2 . This is a natural normalization for discussing the renormalization of *open* intersecting lines (see [26–28]) and makes Γ_{cross} more symmetric. However it does not coincide with the normalization used in some of the literature in which they discuss the renormalization of closed loops. We will later translate the final result to such a normalization.

The last step is to compute \mathbb{W}_0 . Let us first consider $\langle \mathcal{W}_{tt} \rangle$. Since both intersections are resolved, it coincides with a correlator of two disconnected loops. Thus, setting $A_1 = 2(\pi + \theta)$ and $A_2 = 2(\pi - \theta)$ in (2.46), we get

$$\langle \mathcal{W}_{tt} \rangle|_{\phi=\theta} = \left\langle \oint_{\mathcal{C}_1 \prec \mathcal{C}_2} \frac{du_1}{8\pi^2 g^2} \frac{du_2}{8\pi^2 g^2} \bar{\Delta}(u_1, u_2) f_{2(\pi+\theta)}(u_1) f_{2(\pi-\theta)}(u_2) \right\rangle_M. \quad (4.26)$$

Using the result in the literature, we can compute its large N limit as¹⁸

$$\langle \mathcal{W}_{tt} \rangle|_{\phi=\theta} \stackrel{N \rightarrow \infty}{=} \left(\frac{\mathcal{I}_1^\theta}{2\pi g_\theta} \right)^2 + \frac{\pi g_\theta \mathcal{I}_1^\theta \mathcal{I}_2^\theta}{3N^2} + \frac{1}{N^2} \sum_{k=1}^{\infty} \frac{k(\mathcal{I}_k^\theta)^2}{(\rho_\theta)^{2k}}. \quad (4.27)$$

Second, $\langle \mathcal{W}_{ti} \rangle (= \langle \mathcal{W}_{it} \rangle)$ is a single-intersection loop with areas $A_1 = 2(\pi + \theta)$ and $A_2 = 2(\pi - \theta)$ (or equivalently, a figure-eight loop with areas $\bar{A}_1 = \bar{A}_2 = 2(\pi - \theta)$). We thus get from (3.31)

$$\langle \mathcal{W}_{ti} \rangle|_{\phi=\theta} = \frac{4\pi g^2 i}{N} \left\langle \oint_{\mathcal{C}_1 \prec \mathcal{C}_2} \frac{du_1}{8\pi^2 g^2} \frac{du_2}{8\pi^2 g^2} \bar{\Delta}(u_1, u_2) \frac{f_{2(\pi+\theta)}(u_1) f_{2(\pi-\theta)}(u_2)}{u_1 - u_2} \right\rangle_M. \quad (4.28)$$

Here the extra factor $1/N$ comes from the normalization that we adopted. The large N limit can be computed from (3.42) as

$$\langle \mathcal{W}_{ti} \rangle|_{\phi=\theta} \stackrel{N \rightarrow \infty}{=} \frac{1}{2\pi N} \left(\frac{\mathcal{I}_0^\theta \mathcal{I}_1^\theta}{g_\theta} + \sum_{k=1}^{\infty} \frac{\mathcal{I}_k^\theta \mathcal{I}_{k+1}^\theta}{g} \left(\rho_\theta^{-2k-1} + (-1)^k \frac{\rho_\theta - \rho_\theta^{-1}}{2} \right) \right). \quad (4.29)$$

Finally, $\langle \mathcal{W}_{ii} \rangle$ is a two-intersection loop which we computed in (3.56). Setting $A_1 = 2(\pi + \theta)$, $A_2 = 2\pi$ and $A_3 = 2\theta$, we get

$$\begin{aligned} \langle \mathcal{W}_{ii} \rangle|_{\phi=\theta} &= \left\langle \oint_{\mathcal{C}_1 \prec \mathcal{C}_2} \frac{du_1}{8\pi^2 g^2} \frac{du_2}{8\pi^2 g^2} \bar{\Delta} f_{2\pi}(u_1) f_{2\pi}(u_2) \right\rangle_M \\ &+ \frac{(4\pi g^2)^2}{N^2} \left\langle \oint_{\mathcal{C}_1 \prec \mathcal{C}_2} \frac{du_1}{8\pi^2 g^2} \frac{du_2}{8\pi^2 g^2} \bar{\Delta} \frac{f_{2\pi}(u_1) f_{2\pi}(u_2) - f_{2(\pi+\theta)}(u_1) f_{2(\pi-\theta)}(u_2)}{(u_1 - u_2)^2} \right\rangle_M. \end{aligned} \quad (4.30)$$

The large N limit can be computed from (3.59), and the result reads

$$\langle \mathcal{W}_{ii} \rangle|_{\phi=\theta} \stackrel{N \rightarrow \infty}{=} \left(\frac{\mathcal{I}_1^0}{2\pi g} \right)^2 + \frac{g\pi \mathcal{I}_1^0 \mathcal{I}_2^0}{3N^2} + \sum_{k=1}^{\infty} \frac{k [(\rho_\theta^{-2k} - (-1)^k) (\mathcal{I}_k^\theta)^2 + (-1)^k (\mathcal{I}_k^0)^2]}{N^2}. \quad (4.31)$$

Note that these expectation values satisfy the following relation (at finite N)

$$\partial_\theta \langle \mathcal{W}_{ii} \rangle|_{\phi=\theta} = -\frac{8\pi g^2}{N} \langle \mathcal{W}_{ti} \rangle|_{\phi=\theta}, \quad \partial_\theta \langle \mathcal{W}_{ti} \rangle|_{\phi=\theta} = -\frac{8\pi g^2}{N} \langle \mathcal{W}_{tt} \rangle|_{\phi=\theta}. \quad (4.32)$$

They are simply the loop equations written in terms of θ -derivatives, but one can also verify them directly from (4.26), (4.28) and (4.30).

¹⁸The result (4.27) can be obtained from (3.57) by setting $A_1 - A_3 = 2(\pi + \theta)$ and $A_2 = 2(\pi - \theta)$.

These expressions, together with the relation (4.25), give the exact cross anomalous dimension in the near BPS limit of the $U(N)$ theory. Using the relations (4.32), we get

$$\gamma_{\text{cross}} = \frac{1}{\det \mathbb{W}_0} \left(\begin{array}{cc} 0 & -\frac{4\pi g^2}{N} \det \mathbb{W}_0 \\ -\frac{\langle \mathcal{W}_{ti} \rangle \partial_\theta \langle \mathcal{W}_{tt} \rangle}{2} - \frac{4\pi g^2 \langle \mathcal{W}_{tt} \rangle^2}{N} & \frac{\langle \mathcal{W}_{ii} \rangle \partial_\theta \langle \mathcal{W}_{tt} \rangle}{2} + \frac{4\pi g^2 \langle \mathcal{W}_{ti} \rangle \langle \mathcal{W}_{tt} \rangle}{N} \end{array} \right) \Big|_{\phi=\theta}. \quad (4.33)$$

Note in particular that the entries in the first row are 0 and $-4\pi g^2/N$ at all orders in λ and N . Expanding the result at large N , we get

$$\gamma_{\text{cross}} \stackrel{N \rightarrow \infty}{=} \left(\begin{array}{cc} 0 & -\frac{4\pi g^2}{N} \\ -\frac{4\pi g^2 h_1 + h_0 h_2}{N} & h_0 + \frac{4\pi g^2 h_2 + \frac{h_0(h_2)^2}{h_1} - h_0 h_3 + h_4}{N^2} \end{array} \right), \quad (4.34)$$

with

$$\begin{aligned} h_0 &= \frac{4\pi\theta g_\theta}{\theta^2 - \pi^2} \frac{\mathcal{I}_2^\theta}{\mathcal{I}_1^\theta}, & h_1 &= \left(\frac{g\mathcal{I}_1^\theta}{g_\theta \mathcal{I}_1^0} \right)^2, \\ h_2 &= 2\pi \left(\frac{g}{\mathcal{I}_1^0} \right)^2 \left(\frac{\mathcal{I}_0^\theta \mathcal{I}_1^\theta}{g_\theta} + \sum_{k=1}^{\infty} \frac{\mathcal{I}_k^\theta \mathcal{I}_{k+1}^\theta}{g} \left(\rho_\theta^{-2k-1} + (-1)^k \frac{\rho_\theta - \rho_\theta^{-1}}{2} \right) \right), \\ h_3 &= \left(\frac{2\pi g_\theta}{\mathcal{I}_1^\theta} \right)^2 \left(\frac{g\pi \mathcal{I}_1^0 \mathcal{I}_2^0}{3} + \sum_{k=1}^{\infty} k \left[(\rho_\theta^{-2k} - (-1)^k) (\mathcal{I}_k^\theta)^2 + (-1)^k (\mathcal{I}_k^0)^2 \right] \right), \\ h_4 &= \left(\frac{2\pi g_\theta}{\mathcal{I}_1^\theta} \right)^2 \sum_{k=1}^{\infty} \frac{k}{2} \partial_\theta \left[(\rho_\theta^{-2k} - (-1)^k) (\mathcal{I}_k^\theta)^2 \right]. \end{aligned} \quad (4.35)$$

Here h_0 is related to the Bremsstrahlung function $B(\lambda)$ in [24] by

$$h_0 = \frac{4\pi^2\theta}{\theta^2 - \pi^2} B(16\pi^2 g_\theta^2). \quad (4.36)$$

The eigenvalues (γ_\pm) of γ_{cross} are given (up to $O(1/N^2)$) by

$$\begin{aligned} \gamma_+ &= h_0 + \frac{1}{N^2} \left(\frac{h_0(h_2)^2}{h_1} + h_0 h_3 + h_4 + 8\pi g^2 h_2 + \frac{16\pi^2 g^4 h_1}{h_0} \right), \\ \gamma_- &= -\frac{1}{N^2} \left(4\pi g^2 h_2 + \frac{16\pi^2 g^4 h_1}{h_0} \right). \end{aligned} \quad (4.37)$$

4.4 $U(1)$ factor and weak- and strong-coupling expansions

We now expand our results and compare them with the perturbative data. However, since the results in the literature are for the $SU(N)$ gauge group, we first need to strip off the $U(1)$ factor from our results, which are for the $U(N)$ gauge group. This can be done by computing the expectation values in the $U(1)$ theory since the Wilson loop in the $U(N)$ theory factorizes as

$$\mathcal{W}_{U(N)} = \mathcal{W}_{U(1)} \mathcal{W}_{SU(N)}. \quad (4.38)$$

Since the $U(1)$ theory is free, the computation is rather straightforward. In addition, as the gauge group is Abelian, the path-ordering is unnecessary and all the four entries of \mathbb{W} become identical. The result can be read off from the Appendix A of [16], or from the two-matrix model in [17] specialized to $U(1)$. For the two disconnected loops with areas defined as in figure 3, this gives

$$\langle \mathcal{W}_1 \mathcal{W}_2 \rangle|_{U(1)} = \exp \left(\frac{g^2}{N^2} \frac{4\pi(4\pi - A_1 + A_2) - (4\pi - A_1 - A_2)^2}{2} \right). \quad (4.39)$$

Setting $A_1 = 2(\pi + \theta)$ and $A_2 = 2(\pi - \theta)$, we get

$$\langle \mathcal{W}_{tt} \rangle|_{U(1)} = \langle \mathcal{W}_{ti} \rangle|_{U(1)} = \langle \mathcal{W}_{it} \rangle|_{U(1)} = \langle \mathcal{W}_{ii} \rangle|_{U(1)} = e^{\frac{8\pi^2 g^2}{N^2} (1 - \frac{\theta}{\pi})} (=: w_{U(1)}) . \quad (4.40)$$

We then obtain

$$\gamma_{\text{cross}}^{\text{SU}(N)} = \gamma_{\text{cross}} - \frac{\partial_{\theta} w_{U(1)}}{2w_{U(1)}} \mathbf{1} = \gamma_{\text{cross}} + \frac{4\pi g^2}{N^2} \mathbf{1}, \quad (4.41)$$

where γ_{cross} is the result for the $U(N)$ theory (4.25) and $\mathbf{1}$ is the 2×2 identity matrix.

Weak coupling Expanding (4.25) and (4.41) at weak coupling, we get the following result for γ_{cross} up to three loops:

$$\begin{aligned} \gamma_{\text{cross}}^{\text{SU}(N)} &= g^2 \gamma_{(1)} + g^4 \gamma_{(2)} + g^6 \gamma_{(3)} + \dots, \\ \gamma_{(1)} &= \begin{pmatrix} \frac{4\pi}{N^2} & -\frac{4\pi}{N} \\ \frac{4(\theta-\pi)}{N} & -4\theta + \frac{4\pi}{N^2} \end{pmatrix}, \quad \gamma_{(2)} = \begin{pmatrix} 0 & 0 \\ \frac{8\theta(\theta-\pi)(\theta-5\pi)}{3N} & \frac{8\theta(\pi^2-\theta^2)}{3} + \frac{16\pi\theta(\theta-\pi)}{N^2} \end{pmatrix}, \\ \gamma_{(3)} &= \begin{pmatrix} 0 & 0 \\ \frac{8(\theta-\pi)\theta(5\pi^3+\pi^2\theta-\pi\theta^2+\theta^3)}{3N} & -\frac{8\theta(\pi^2-\theta^2)^2}{3} + \frac{16\pi\theta(\theta-\pi)(\pi^2-9\pi\theta+5\theta^2)}{3N^2} \end{pmatrix}. \end{aligned} \quad (4.42)$$

Closed-loop normalization As mentioned below (4.25), the normalization we used is suited for the renormalization of open intersecting lines. To translate our result into the normalization commonly used for the renormalization of closed loops, we simply need to perform the following conjugation as explained in [26]¹⁹

$$\Gamma_{\text{cross}}^{\text{closed}} = S \Gamma_{\text{cross}} S^{-1}, \quad \gamma_{\text{cross}}^{\text{closed}} = S \gamma_{\text{cross}} S^{-1}, \quad (4.43)$$

with $S := \text{diag}(\sqrt{N}, 1/\sqrt{N})$. We then get

$$\begin{aligned} \gamma_{\text{cross}}^{\text{SU}(N), \text{closed}} &= g^2 \gamma_{(1)}^{\text{closed}} + g^4 \gamma_{(2)}^{\text{closed}} + g^6 \gamma_{(3)}^{\text{closed}} + \dots, \\ \gamma_{(1)}^{\text{closed}} &= \begin{pmatrix} \frac{4\pi}{N^2} & -4\pi \\ \frac{4(\theta-\pi)}{N^2} & -4\theta + \frac{4\pi}{N^2} \end{pmatrix}, \quad \gamma_{(2)}^{\text{closed}} = \begin{pmatrix} 0 & 0 \\ \frac{8\theta(\theta-\pi)(\theta-5\pi)}{3N^2} & \frac{8\theta(\pi^2-\theta^2)}{3} + \frac{16\pi\theta(\theta-\pi)}{N^2} \end{pmatrix}, \\ \gamma_{(3)}^{\text{closed}} &= \begin{pmatrix} 0 & 0 \\ \frac{8(\theta-\pi)\theta(5\pi^3+\pi^2\theta-\pi\theta^2+\theta^3)}{3N^2} & -\frac{8\theta(\pi^2-\theta^2)^2}{3} + \frac{16\pi\theta(\theta-\pi)(\pi^2-9\pi\theta+5\theta^2)}{3N^2} \end{pmatrix}. \end{aligned} \quad (4.44)$$

¹⁹In [26], Γ_{cross} and $\Gamma_{\text{cross}}^{\text{closed}}$ were denoted as $\hat{\Gamma}_{\text{cross}}$ and Γ_{cross} respectively.

$\gamma_{(1,2)}^{\text{closed}}$ are in perfect agreement²⁰ with the near-BPS limit of the two-loop results in [26]. It would be interesting to perform a direct three-loop computation and reproduce $\gamma_{(3)}^{\text{closed}}$.

Strong coupling The strong coupling limit of γ_{cross} can be computed from the results for intersecting loops in section 3.2. The result in the planar limit reads

$$\begin{aligned}\mathbb{W}_0 &\sim \begin{pmatrix} (c_0 + \frac{c_1}{N^2})e^{8\pi g} + \frac{c_2(\theta)e^{8\pi g\theta}}{N^2} & \frac{c_3(\theta)e^{8\pi g\theta}}{N} \\ \frac{c_3(\theta)e^{8\pi g\theta}}{N} & c_4(\theta)e^{8\pi g\theta} \end{pmatrix}, \\ \mathbb{W}_0^{-1} &\sim \begin{pmatrix} \frac{e^{-8\pi g}}{c_0} & -\frac{c_3(\theta)e^{-8\pi g}}{c_0 c_4(\theta)N} \\ -\frac{c_3(\theta)e^{-8\pi g}}{c_0 c_4(\theta)N} & \frac{e^{-8\pi g\theta}}{c_4(\theta)} \end{pmatrix},\end{aligned}\tag{4.45}$$

where c_0 and c_1 are θ -independent while c_2 - c_4 are θ -dependent prefactors, among which c_3 and c_4 are relevant for the analysis:

$$c_3(\theta) = -\frac{1}{32\pi^2(g_\theta^2\theta)} (1 + O(g^{-1})) , \quad c_4(\theta) = \frac{1}{8\pi^2(g_\theta)^3} (1 + O(g^{-1})) .\tag{4.46}$$

We then get the following result in the planar limit:

$$\gamma_{\text{cross}}^{\text{SU(N),closed}} = 4\pi\partial_\theta g_\theta \begin{pmatrix} 0 & \frac{c_3}{c_4} \\ 0 & 1 \end{pmatrix} + \frac{1}{2} \begin{pmatrix} 0 & \frac{\partial_\theta c_3}{\partial_\theta c_4} \\ 0 & \frac{c_4}{c_4} \end{pmatrix} + O(N^{-2}).\tag{4.47}$$

The leading strong-coupling answer for the lower-diagonal component $-4\pi\partial_\theta g_\theta$ reproduces the prediction made in [26] using the classical worldsheet. By contrast, the leading strong-coupling answer for the upper-right component is given by

$$4\pi\partial_\theta g_\theta \frac{c_3}{c_4} \sim \frac{g^2}{\pi},\tag{4.48}$$

and does not match with the one in [26], which predicts the same answer as the lower-diagonal component, $4\pi\partial_\theta g_\theta$. This however does not immediately imply contradiction: As is well-known, the individual matrix elements of the anomalous dimension depend on the choice of the basis of operators. It is likely that the choice we made here for supersymmetric localization is different from the choice implicitly made in the analysis of the classical worldsheet. To avoid such ambiguities, we should compare the eigenvalues of the anomalous dimension matrix, which in fact agree with the ones in [26]. It would be important to understand this point further and also perform a comparison at the nonplanar level.

5 Conclusion

In this paper, we computed the expectation values of intersecting 1/8 BPS Wilson loops in $\mathcal{N} = 4$ SYM at finite λ and N using supersymmetric localization and the loop equation. The

²⁰ [26] uses a slightly non-standard convention in which the cross anomalous dimension is defined with an extra minus sign. (This can be seen by comparing (4.1) of our paper and (2.3) of [26]). Thus, to compare with our results, we need to consider $-\Gamma_{\text{cross}}$ in [26].

results are given by a coupled system of the Gaussian matrix model and multiple contour integrals, which in the planar limit give an infinite sum of products of modified Bessel functions. Applying the formalism to near-BPS limits of the cross anomalous dimension, we reproduced the perturbative data in [26].

The main message of this paper is that the loop equation provides a powerful computational tool in $\mathcal{N} = 4$ SYM when combined with localization.²¹ It would be interesting to explore the connection with other nonperturbative techniques such as integrability and the conformal bootstrap²²: The intersecting lightlike Wilson lines were studied in the planar limit [50] from integrability by the pentagon OPE [51]. However the relation to the loop equation was not explored. Studying them through the lens of the loop equation may lead to stronger results, or at least would lead to a deeper understanding of the pentagon OPE.

The $1/2$ BPS Wilson loop in $\mathcal{N} = 4$ SYM is an example of a conformal defect [57–59]. The insertion of $F_{\mu\nu}$ —which plays the central role in the derivation of the loop equation—is a displacement operator, which is present in any conformal defect. Rephrasing the loop equation in the language of the defect CFT may allow us to use it as a dynamical input²³ for the conformal bootstrap. This would be perhaps useful for the nonsupersymmetric Wilson line discussed in [60–62]. Of course, in the absence of supersymmetric localization, one would need to study in this case the loop equation in the 4d gauge theory. Another direction is to analyze intersecting conformal defects in general CFTs. For the case of two intersecting 1d defects, one should be able to interpret them as a conformal two-point function of intersections as discussed in section 4.2.

Regarding the cross anomalous dimension, the simplest next step would be to generalize our computation to multiple lines intersecting at a point. This would shed light on the structure of the soft anomalous dimension of multileg amplitudes, studied for instance in [63]. Of course, our analysis only applies to a small angle (or near-BPS) limit but it might be possible to combine it with the bootstrap approach in [64] and constrain the full answer.

Another interesting direction is to perform the computation in different setups. For instance, the exact Bremsstrahlung function in $\mathcal{N} = 2$ SCFT was computed in [65, 66]. Generalizing it to the small angle limit of the cross anomalous dimension is an important problem. It would also be interesting to study the ladder limit of the Wilson loop in $\mathcal{N} = 4$ SYM, in which the R-symmetry angle θ is sent to $i\infty$ while the combination $\hat{\lambda} := \lambda e^{-i\theta}$ is held fixed. This limit selects the ladder diagrams which can be resummed analytically [67–72]. Last but not least, it is important to further study the cross anomalous dimension in perturbation theory. In particular, it would be desirable to generalize the result for the supersymmetric Wilson lines in [26] to nonsupersymmetric Wilson lines.

Acknowledgement

We thank Jiaqi Jiang for collaboration on a related topic, and Hagen Münkler for discussions and comments on the draft. SK thanks Lance Dixon, Grigory Korchemsky, Enrico Herrmann,

²¹See [52–54] for previous attempts to analyze the loop equation in $\mathcal{N} = 4$ SYM and gauge/string duality.

²²See [55, 56] for interesting proposals on (different) bootstrap approaches to the loop equation.

²³Here we have in mind the loop equation for the *non-intersecting line*, for which the right hand side of the loop equation vanishes.

and Ian Moulton for discussions on the cross anomalous dimension. We thank CERN for hospitality during completion of this work. The work of SG is supported in part by the US NSF under Grants No. PHY-1620542 and PHY-1914860. The work of SK is supported by DOE grant number DE-SC0009988.

A Infinite Sum of Modified Bessel Functions

In this appendix, we derive identities for the infinite sum of modified Bessel functions and apply it to (3.44) to rewrite it in a more symmetric form. The starting point is the integral representation

$$I_n(z) = \oint \frac{dx}{2\pi i x} \frac{e^{\frac{z}{2}(x+1/x)}}{x^n}. \quad (\text{A.1})$$

We then rescale the integration variable $x \rightarrow \alpha x$ to get

$$I_n(z) = \frac{1}{\alpha^n} \oint \frac{dx}{2\pi i x} \frac{e^{\frac{z}{2}(\alpha x + 1/(\alpha x))}}{x^n}. \quad (\text{A.2})$$

We now factorize the exponential into two pieces

$$\exp\left[\frac{z}{2}\left(\alpha x + \frac{1}{\alpha x}\right)\right] = \exp\left[\frac{z_1}{2}\left(x + \frac{1}{x}\right)\right] \times \exp\left[\frac{z_2}{2}\left(\beta x + \frac{1}{\beta x}\right)\right], \quad (\text{A.3})$$

with

$$z = \sqrt{z_1^2 + z_2^2 + \left(\beta + \frac{1}{\beta}\right) z_1 z_2}, \quad \alpha = \sqrt{\frac{z_1 + z_2 \beta}{z_1 + z_2 \beta^{-1}}}. \quad (\text{A.4})$$

and use the generating function representation for each exponential:

$$e^{\frac{y}{2}(x+1/x)} = \sum_{k=-\infty}^{\infty} I_k(y) y^k. \quad (\text{A.5})$$

After performing the integral of x , we get

$$I_n(z) = \frac{1}{\alpha^n} \sum_{k=-\infty}^{\infty} \beta^k I_{n-k}(z_1) I_k(z_2). \quad (\text{A.6})$$

Specifying n to be 1 and using $I_{-k} = I_k$, we get the identity

$$I_1(z) = \frac{1}{\alpha} \sum_{k=0}^{\infty} \beta^{k+1} I_k(z_1) I_{k+1}(z_2) + \beta^{-k} I_{k+1}(z_1) I_k(z_2). \quad (\text{A.7})$$

Now applying this identity (A.7), we can exchange $\bar{A}_{1,2}$ in (3.44):

$$\langle \mathcal{W}_{\text{figure-eight}} \rangle \stackrel{N \rightarrow \infty}{=} \frac{\mathcal{I}_0^{\bar{a}_2} \mathcal{I}_1^{\bar{a}_1}}{2\pi g_{\bar{a}_1}} + \sum_{k=1}^{\infty} \frac{\rho_{\bar{a}_2}^k \mathcal{I}_k^{\bar{a}_2}}{4\pi g} \left[\left(\rho_{\bar{a}_1}^{k+1} + \frac{(-1)^k}{\rho_{\bar{a}_1}^{k+1}} \right) \mathcal{I}_{k+1}^{\bar{a}_1} + \left(\rho_{\bar{a}_1}^{k-1} + \frac{(-1)^k}{\rho_{\bar{a}_1}^{k-1}} \right) \mathcal{I}_{k-1}^{\bar{a}_1} \right]. \quad (\text{A.8})$$

It is also possible to make it manifestly symmetric under $\bar{A}_1 \leftrightarrow \bar{A}_2$:

$$\langle \mathcal{W}_{\text{figure-eight}} \rangle \stackrel{N \rightarrow \infty}{=} \frac{I_1^{\frac{\bar{a}_1 - \bar{a}_2}{2}}(2g)}{4\pi g} + \frac{1}{2\pi g} \sum_{k=1}^{\infty} (I_{k+1}^{\bar{a}_1}(g) I_k^{\bar{a}_2}(g) + I_{k+1}^{\bar{a}_2}(g) I_k^{\bar{a}_1}(g)) , \quad (\text{A.9})$$

Here $I^\theta(g)$ is the modified Bessel function introduced in [42],

$$I_k^\theta(g) := \frac{I_k(4\pi g_\theta)}{2} \left[\left(\frac{\pi + \theta}{\pi - \theta} \right)^{\frac{k}{2}} - (-1)^k \left(\frac{\pi - \theta}{\pi + \theta} \right)^{\frac{k}{2}} \right] . \quad (\text{A.10})$$

B Cross Anomalous Dimension of Two Touching Lines

In this appendix, we compute the cross anomalous dimension of two touching Wilson lines. The basic strategy is the same as in section 4: We map it to a sphere, view it as two-point functions of intersections and differentiate it with respect to the angle θ .

In this case, the analogue of (4.17) is given by

$$\bar{\mathbb{W}}_0 = \left(\begin{array}{cc} \langle \mathcal{W}_{11} \rangle & \langle \mathcal{W}_{12} \rangle \\ \langle \mathcal{W}_{21} \rangle & \langle \mathcal{W}_{22} \rangle \end{array} \right) \Big|_{\phi=\theta} , \quad (\text{B.1})$$

where \mathcal{W}_{ij} denotes a Wilson loop whose intersections at the north and the south poles are resolved into configurations i and j in figure 13-(b). The formula (4.25) applies also to this case and the computation boils down to computing the BPS loops $\langle \mathcal{W}_{ij} \rangle|_{\phi=\theta}$. The main difference from section 4 is that all the relevant loops are non-intersecting and one can simply use the results in the literature.

Let us first consider $\langle \mathcal{W}_{11} \rangle$. It corresponds to two oppositely-oriented Wilson loops with areas $A_1 = 4\pi - 2\theta$ and $A_2 = 2\theta$. Using the result in [17], we find²⁴

$$\langle \mathcal{W}_{11} \rangle|_{\phi=\theta} = \left(\frac{\mathcal{I}_1^{\pi-\theta}}{2\pi g_{\pi-\theta}} \right)^2 + \frac{\pi g_{\pi-\theta} \mathcal{I}_1^{\pi-\theta} \mathcal{I}_2^{\pi-\theta}}{3N^2} + \frac{1}{N^2} \sum_{k=1}^{\infty} \frac{k(-1)^k (\mathcal{I}_k^{\pi-\theta})^2}{(\rho_{\pi-\theta})^{2k}} + O(1/N^4) . \quad (\text{B.2})$$

On the other hand, \mathcal{W}_{12} and \mathcal{W}_{21} are single Wilson loops with areas 4θ and $4(\pi - \theta)$ respectively. They have the same expectation values given by²⁵

$$\langle \mathcal{W}_{12} \rangle|_{\phi=\theta} = \langle \mathcal{W}_{21} \rangle|_{\phi=\theta} = \frac{1}{N} \left(\frac{\mathcal{I}_1^{2\theta-\pi}}{2\pi g_{2\theta-\pi}} + \frac{\pi^2 g_{2\theta-\pi}^2 \mathcal{I}_2^{2\theta-\pi}}{3N^2} \right) + O(1/N^4) . \quad (\text{B.3})$$

Finally \mathcal{W}_{22} corresponds to two oppositely-oriented loops with areas $A_1 = 2(\pi + \theta)$ and $A_2 = 2(\pi - \theta)$. We then have

$$\langle \mathcal{W}_{22} \rangle|_{\phi=\theta} = \left(\frac{\mathcal{I}_1^\theta}{2\pi g_\theta} \right)^2 + \frac{\pi g_\theta \mathcal{I}_1^\theta \mathcal{I}_2^\theta}{3N^2} + \frac{1}{N^2} \sum_{k=1}^{\infty} \frac{k(-1)^k (\mathcal{I}_k^\theta)^2}{(\rho_\theta)^{2k}} + O(1/N^4) . \quad (\text{B.4})$$

²⁴In this appendix, we focus on the large N limit for simplicity. The result at finite N can be obtained using matrix models in [16].

²⁵As in section 4, here we normalized the Wilson loops by dividing by a common factor N^2 . This is the origin of the extra factor of $1/N$ in (B.2).

From $\bar{\mathbb{W}}_0$, the near-BPS limit of the cross anomalous dimension $\bar{\Gamma}_{\text{cross}} = (\phi - \theta)\bar{\gamma}_{\text{cross}} + O((\phi - \theta)^2)$ can be computed by $\bar{\gamma}_{\text{cross}} = \frac{1}{2}(\partial_\theta \bar{\mathbb{W}}_0) \cdot (\bar{\mathbb{W}}_0)^{-1}$. The result reads

$$\bar{\gamma}_{\text{cross}} = \begin{pmatrix} -\bar{h}_0^- + \frac{1}{N^2} \left(\bar{h}_0^- \bar{h}_1^- - \frac{\bar{h}_2^-}{2} - (\bar{h}_0^+ + \bar{h}_0^-) \bar{h}_3^- \bar{h}_3 \right) & \frac{(\bar{h}_0^+ + \bar{h}_0^-) \bar{h}_3}{N} \\ \frac{(\bar{h}_0^+ - \bar{h}_0^-) \bar{h}_3}{N} & \bar{h}_0 + \frac{1}{N^2} \left(-\bar{h}_0 \bar{h}_1 + \frac{\bar{h}_2}{2} - (\bar{h}_0^+ - \bar{h}_0^-) \bar{h}_3^- \bar{h}_3 \right) \end{pmatrix}, \quad (\text{B.5})$$

with $\bar{h}_k := \bar{h}_k(\theta)$, $\bar{h}_k^- := \bar{h}_k(\pi - \theta)$ and $\bar{h}_k^+ := \bar{h}_k(2\theta - \pi)$ and

$$\begin{aligned} \bar{h}_0(\theta) &= \frac{4\pi\theta g_\theta}{\theta^2 - \pi^2} \frac{\mathcal{I}_2^\theta}{\mathcal{I}_1^\theta}, & \bar{h}_1(\theta) &= \left(\frac{\mathcal{I}_1^\theta}{2\pi g_\theta} \right)^2 \left[\frac{\pi g_\theta \mathcal{I}_1^\theta \mathcal{I}_2^\theta}{3} + \sum_{k=1}^{\infty} \frac{k(-1)^k (\mathcal{I}_k^\theta)^2}{(\rho_\theta)^{2k}} \right], \\ \bar{h}_2(\theta) &= \frac{2\pi g_\theta^2 \mathcal{I}_1^{2\theta-\pi}}{(\mathcal{I}_1^\theta)^2}, & \bar{h}_3(\theta) &= \left(\frac{\mathcal{I}_1^\theta}{2\pi g_\theta} \right)^2 \partial_\theta \left[\frac{\pi g_\theta \mathcal{I}_1^\theta \mathcal{I}_2^\theta}{3} + \sum_{k=1}^{\infty} \frac{k(-1)^k (\mathcal{I}_k^\theta)^2}{(\rho_\theta)^{2k}} \right]. \end{aligned} \quad (\text{B.6})$$

The eigenvalue ($\bar{\gamma}_\pm$) are given by

$$\begin{aligned} \bar{\gamma}_+ &= \bar{h}_0 + \frac{(\bar{h}_0 + \bar{h}_0^-)(-2\bar{h}_0 \bar{h}_1 + \bar{h}_2^-) + 2(\bar{h}_0 - \bar{h}_0^-)^2 \bar{h}_3 \bar{h}_3^-}{2N^2(\bar{h}_0 + \bar{h}_0^-)}, \\ \bar{\gamma}_- &= -\bar{h}_0^- + \frac{(\bar{h}_0 + \bar{h}_0^-)(2\bar{h}_0^- \bar{h}_1^- - \bar{h}_2^-) - 2(\bar{h}_0^- + \bar{h}_0^+)^2 \bar{h}_3 \bar{h}_3^-}{2N^2(\bar{h}_0 + \bar{h}_0^-)}. \end{aligned} \quad (\text{B.7})$$

To perform a comparison with the results in [26], one needs to consider the $\text{SU}(N)$ theory by stripping off the $\text{U}(1)$ factor

$$\bar{\gamma}_{\text{cross}}^{\text{SU}(N)} = \bar{\gamma}_{\text{cross}} - \frac{\partial_\theta \bar{w}_{\text{U}(1)}}{2\bar{w}_{\text{U}(1)}} \mathbf{1}. \quad (\text{B.8})$$

Here $\bar{w}_{\text{U}(1)}$ is the $\text{U}(1)$ factor which in this case is the expectation value of the Wilson loop with area 4θ (see [16]),

$$\bar{w}_{\text{U}(1)} = \exp \left(\frac{8g^2\theta(\pi - \theta)}{N^2} \right). \quad (\text{B.9})$$

Converting the result to the closed-loop normalization by $\bar{\gamma}_{\text{cross}}^{\text{closed}} = S \bar{\gamma}_{\text{cross}} S^{-1}$ with $S = \text{diag}(\sqrt{N}, 1/\sqrt{N})$, and expanding the result at weak coupling, we get

$$\bar{\gamma}_{\text{cross}}^{\text{SU}(N), \text{closed}} = g^2 \bar{\gamma}_{(1)}^{\text{closed}} + g^4 \bar{\gamma}_{(2)}^{\text{closed}} + g^6 \bar{\gamma}_{(3)}^{\text{closed}} + \dots, \quad (\text{B.10})$$

$$\bar{\gamma}_{(1)}^{\text{closed}} = -4 \begin{pmatrix} (\theta - \pi) + \frac{\pi - 2\theta}{N^2} & \theta \\ \frac{\theta - \pi}{N^2} & \theta + \frac{\pi - 2\theta}{N^2} \end{pmatrix},$$

$$\bar{\gamma}_{(2)}^{\text{closed}} = -\frac{8}{3} \begin{pmatrix} \theta(\theta - \pi)(\theta - 2\pi) + \frac{2\theta(\pi^2 - \theta^2)}{N^2} & \theta(\theta - \pi)(\theta + 4\pi) \\ \frac{\theta(\theta - \pi)(\theta - 5\pi)}{N^2} & (\theta^2 - \pi^2) - \frac{2\theta(\theta - \pi)(\theta - 2\pi)}{N^2} \end{pmatrix},$$

$$\bar{\gamma}_{(3)}^{\text{closed}} = -\frac{8}{3} \begin{pmatrix} (\theta - \pi)(\theta - 2\pi)^2\theta^2 + \frac{2\theta(\theta - \pi)(3\pi^3 - 3\pi^2\theta + 5\pi\theta^2 - \theta^3)}{N^2} & \theta(\theta - \pi)(\theta^3 + 2\pi\theta^2 + 2\pi^2\theta - 6\pi^3) \\ \frac{\theta(\theta - \pi)(\pi^3 + 9\pi^2\theta - 5\pi\theta^2 + \theta^3)}{N^2} & \theta(\pi^2 - \theta^2)^2 - \frac{2\theta(\theta - \pi)(4\pi^3 - 4\pi^2\theta + 2\pi\theta^2 + \theta^3)}{N^2} \end{pmatrix}.$$

The results up to two loops reproduce the perturbative computation in [26].

The strong coupling expansion can be obtained from the results in section 3.2. In the planar limit, we have

$$\bar{\mathbb{W}}_0 \sim \begin{pmatrix} \bar{c}_1 e^{8\pi g_{\pi-\theta}} & \frac{\bar{c}_2 e^{4\pi g_{2\theta-\pi}}}{N} \\ \frac{\bar{c}_2 e^{4\pi g_{2\theta-\pi}}}{N} & \bar{c}_3 e^{8\pi g_\theta} \end{pmatrix}, \quad \bar{\mathbb{W}}_0^{-1} \sim \begin{pmatrix} \frac{e^{-8\pi g_{\pi-\theta}}}{\bar{c}_1} & -\frac{\bar{c}_2 e^{4\pi(g_{2\theta-\pi}-2g_\theta-2g_{\pi-\theta})}}{\bar{c}_1 \bar{c}_3 N} \\ -\frac{\bar{c}_2 e^{4\pi(g_{2\theta-\pi}-2g_\theta-2g_{\pi-\theta})}}{\bar{c}_1 \bar{c}_3 N} & \frac{e^{-8\pi g_\theta}}{\bar{c}_3} \end{pmatrix},$$

where the prefactors all depend on θ and are given (at strong coupling) by

$$\bar{c}_1 = \frac{1}{8\pi^2(g_{\pi-\theta})^3}, \quad \bar{c}_2 = \frac{1}{\pi(2g_{2\theta-\pi})^{3/2}}, \quad \bar{c}_3 = \frac{1}{8\pi^2 g_\theta^3}. \quad (\text{B.11})$$

Then the leading answer at strong coupling is given by

$$\gamma_{\text{cross}}^{\text{SU(N),closed}} = \begin{pmatrix} 4\pi\partial_\theta g_{\pi-\theta} & \frac{2\pi\bar{c}_2}{\bar{c}_3}(\partial_\theta g_{2\theta-\pi} - 2\partial_\theta g_{\pi-\theta})e^{4\pi(g_{2\theta-\pi}-2g_\theta)} \\ 0 & 4\pi\partial_\theta g_\theta \end{pmatrix} + \dots \quad (\text{B.12})$$

As in section 4.4, the diagonal components reproduce the results in [26] while the upper off-diagonal component does not match with the one in [26]. However the off-diagonal component is exponentially suppressed at strong coupling since $g_{2\theta-\pi} < 2g_\theta$. Thus the eigenvalues of the matrix do coincide with the ones in [26]. (See the discussion below (4.48)).

References

- [1] Yu. M. Makeenko and A. A. Migdal, *Exact Equation for the Loop Average in Multicolor QCD*, *Phys. Lett.* **88B** (1979) 135.
- [2] Yu. Makeenko and A. A. Migdal, *Quantum Chromodynamics as Dynamics of Loops*, *Nucl. Phys.* **B188** (1981) 269.
- [3] Y. Makeenko, *Large N gauge theories*, *NATO Sci. Ser. C* **556** (2000) 285 [[hep-th/0001047](#)].
- [4] A. A. Migdal, *Loop Equations and 1/N Expansion*, *Phys. Rept.* **102** (1983) 199.
- [5] V. A. Kazakov and I. K. Kostov, *Nonlinear strings in two-dimensional $U(\infty)$ gauge theory*, *Nucl. Phys.* **B176** (1980) 199.
- [6] V. A. Kazakov, *Wilson loop average for an arbitrary contour in two-dimensional $U(N)$ gauge theory*, *Nucl. Phys.* **B179** (1981) 283.
- [7] D. V. Boulatov, *Wilson loop on a sphere*, *Mod. Phys. Lett.* **A9** (1994) 365 [[hep-th/9310041](#)].
- [8] J.-M. Daul and V. A. Kazakov, *Wilson loop for large N Yang-Mills theory on a two-dimensional sphere*, *Phys. Lett.* **B335** (1994) 371 [[hep-th/9310165](#)].

- [9] V. Pestun, *Localization of gauge theory on a four-sphere and supersymmetric Wilson loops*, *Commun. Math. Phys.* **313** (2012) 71 [[0712.2824](#)].
- [10] V. Pestun, *Localization of the four-dimensional $N=4$ SYM to a two-sphere and $1/8$ BPS Wilson loops*, *JHEP* **12** (2012) 067 [[0906.0638](#)].
- [11] N. Drukker, S. Giombi, R. Ricci and D. Trancanelli, *Wilson loops: From four-dimensional SYM to two-dimensional YM*, *Phys. Rev.* **D77** (2008) 047901 [[0707.2699](#)].
- [12] N. Drukker, S. Giombi, R. Ricci and D. Trancanelli, *Supersymmetric Wilson loops on S^{*3}* , *JHEP* **05** (2008) 017 [[0711.3226](#)].
- [13] J. K. Erickson, G. W. Semenoff and K. Zarembo, *Wilson loops in $N=4$ supersymmetric Yang-Mills theory*, *Nucl. Phys.* **B582** (2000) 155 [[hep-th/0003055](#)].
- [14] N. Drukker and D. J. Gross, *An Exact prediction of $N=4$ SUSYM theory for string theory*, *J. Math. Phys.* **42** (2001) 2896 [[hep-th/0010274](#)].
- [15] S. Giombi and V. Pestun, *Correlators of local operators and $1/8$ BPS Wilson loops on S^{*2} from 2d YM and matrix models*, *JHEP* **10** (2010) 033 [[0906.1572](#)].
- [16] S. Giombi and V. Pestun, *Correlators of Wilson Loops and Local Operators from Multi-Matrix Models and Strings in AdS*, *JHEP* **01** (2013) 101 [[1207.7083](#)].
- [17] S. Giombi, V. Pestun and R. Ricci, *Notes on supersymmetric Wilson loops on a two-sphere*, *JHEP* **07** (2010) 088 [[0905.0665](#)].
- [18] S. Giombi and V. Pestun, *The $1/2$ BPS 't Hooft loops in $N=4$ SYM as instantons in 2d Yang-Mills*, *J. Phys.* **A46** (2013) 095402 [[0909.4272](#)].
- [19] A. Bassetto, L. Griguolo, F. Pucci, D. Seminara, S. Thambyahpillai and D. Young, *Correlators of supersymmetric Wilson-loops, protected operators and matrix models in $N=4$ SYM*, *JHEP* **08** (2009) 061 [[0905.1943](#)].
- [20] A. Bassetto, L. Griguolo, F. Pucci, D. Seminara, S. Thambyahpillai and D. Young, *Correlators of supersymmetric Wilson loops at weak and strong coupling*, *JHEP* **03** (2010) 038 [[0912.5440](#)].
- [21] M. Bonini, L. Griguolo and M. Preti, *Correlators of chiral primaries and $1/8$ BPS Wilson loops from perturbation theory*, *JHEP* **09** (2014) 083 [[1405.2895](#)].
- [22] M. Bonini, L. Griguolo, M. Preti and D. Seminara, *Bremsstrahlung function, leading Lscher correction at weak coupling and localization*, *JHEP* **02** (2016) 172 [[1511.05016](#)].
- [23] S. Cordes, G. W. Moore and S. Ramgoolam, *Lectures on 2-d Yang-Mills theory, equivariant cohomology and topological field theories*, *Nucl. Phys. Proc. Suppl.* **41** (1995) 184 [[hep-th/9411210](#)].

- [24] D. Correa, J. Henn, J. Maldacena and A. Sever, *An exact formula for the radiation of a moving quark in $N=4$ super Yang Mills*, *JHEP* **06** (2012) 048 [[1202.4455](#)].
- [25] S. Giombi and S. Komatsu, *Exact Correlators on the Wilson Loop in $\mathcal{N} = 4$ SYM: Localization, Defect CFT, and Integrability*, *JHEP* **05** (2018) 109 [[1802.05201](#)].
- [26] H. Münkler, *The Cross Anomalous Dimension in Maximally Supersymmetric Yang-Mills Theory*, *JHEP* **10** (2018) 162 [[1805.06448](#)].
- [27] G. P. Korchemsky, *On Near forward high-energy scattering in QCD*, *Phys. Lett.* **B325** (1994) 459 [[hep-ph/9311294](#)].
- [28] I. A. Korchemskaya and G. P. Korchemsky, *High-energy scattering in QCD and cross singularities of Wilson loops*, *Nucl. Phys.* **B437** (1995) 127 [[hep-ph/9409446](#)].
- [29] S. Giombi, J. Jiang and S. Komatsu, *Defect CFT Correlators on the Giant Wilson Loops*, **200x.xxxxx**.
- [30] B. Basso, S. Komatsu and P. Vieira, *Structure Constants and Integrable Bootstrap in Planar $N=4$ SYM Theory*, **1505.06745**.
- [31] Y. Jiang, S. Komatsu, I. Kostov and D. Serban, *Clustering and the Three-Point Function*, *J. Phys.* **A49** (2016) 454003 [[1604.03575](#)].
- [32] T. Fleury and S. Komatsu, *Hexagonalization of Correlation Functions*, *JHEP* **01** (2017) 130 [[1611.05577](#)].
- [33] B. Eden, Y. Jiang, M. de Leeuw, T. Meier, D. le Plat and A. Sfondrini, *Positivity of hexagon perturbation theory*, *JHEP* **11** (2018) 097 [[1806.06051](#)].
- [34] F. Coronado, *Perturbative four-point functions in planar $\mathcal{N} = 4$ SYM from hexagonalization*, *JHEP* **01** (2019) 056 [[1811.00467](#)].
- [35] T. Bargheer, F. Coronado and P. Vieira, *Octagons II: Strong Coupling*, **1909.04077**.
- [36] I. Kostov, V. B. Petkova and D. Serban, *Determinant Formula for the Octagon Form Factor in $N=4$ Supersymmetric Yang-Mills Theory*, *Phys. Rev. Lett.* **122** (2019) 231601 [[1903.05038](#)].
- [37] I. Kostov, V. B. Petkova and D. Serban, *The Octagon as a Determinant*, *JHEP* **11** (2019) 178 [[1905.11467](#)].
- [38] A. V. Belitsky and G. P. Korchemsky, *Exact null octagon*, **1907.13131**.
- [39] M. de Leeuw, B. Eden, D. I. Plat, T. Meier and A. Sfondrini, *Multi-particle finite-volume effects for hexagon tessellations*, **1912.12231**.
- [40] A. V. Belitsky and G. P. Korchemsky, *Octagon at finite coupling*, **2003.01121**.

- [41] S. Giombi and S. Komatsu, *More Exact Results in the Wilson Loop Defect CFT: Bulk-Defect OPE, Nonplanar Corrections and Quantum Spectral Curve*, *J. Phys.* **A52** (2019) 125401 [[1811.02369](#)].
- [42] N. Gromov, F. Levkovich-Maslyuk and G. Sizov, *Analytic Solution of Bremsstrahlung TBA II: Turning on the Sphere Angle*, *JHEP* **10** (2013) 036 [[1305.1944](#)].
- [43] N. Drukker, *1/4 BPS circular loops, unstable world-sheet instantons and the matrix model*, *JHEP* **09** (2006) 004 [[hep-th/0605151](#)].
- [44] V. Forini, A. A. Tseytlin and E. Vescovi, *Perturbative computation of string one-loop corrections to Wilson loop minimal surfaces in $AdS_5 \times S^5$* , *JHEP* **03** (2017) 003 [[1702.02164](#)].
- [45] D. Medina-Rincon, A. A. Tseytlin and K. Zarembo, *Precision matching of circular Wilson loops and strings in $AdS_5 \times S^5$* , *JHEP* **05** (2018) 199 [[1804.08925](#)].
- [46] T. Becher and M. Neubert, *Infrared singularities of scattering amplitudes in perturbative QCD*, *Phys. Rev. Lett.* **102** (2009) 162001 [[0901.0722](#)].
- [47] E. Gardi and L. Magnea, *Factorization constraints for soft anomalous dimensions in QCD scattering amplitudes*, *JHEP* **03** (2009) 079 [[0901.1091](#)].
- [48] T. Becher and M. Neubert, *On the Structure of Infrared Singularities of Gauge-Theory Amplitudes*, *JHEP* **06** (2009) 081 [[0903.1126](#)].
- [49] L. J. Dixon and I. Esterlis, *All orders results for self-crossing Wilson loops mimicking double parton scattering*, *JHEP* **07** (2016) 116 [[1602.02107](#)].
- [50] S. Caron-Huot, L. J. Dixon, F. Dulat, M. von Hippel, A. J. McLeod and G. Papathanasiou, *Six-Gluon amplitudes in planar $\mathcal{N} = 4$ super-Yang-Mills theory at six and seven loops*, *JHEP* **08** (2019) 016 [[1903.10890](#)].
- [51] B. Basso, A. Sever and P. Vieira, *Spacetime and Flux Tube S-Matrices at Finite Coupling for $N=4$ Supersymmetric Yang-Mills Theory*, *Phys. Rev. Lett.* **111** (2013) 091602 [[1303.1396](#)].
- [52] N. Drukker, *A new type of loop equations*, *JHEP* **11** (1999) 006 [[hep-th/9908113](#)].
- [53] A. M. Polyakov and V. S. Rychkov, *Gauge field strings duality and the loop equation*, *Nucl. Phys.* **B581** (2000) 116 [[hep-th/0002106](#)].
- [54] A. M. Polyakov and V. S. Rychkov, *Loop dynamics and AdS / CFT correspondence*, *Nucl. Phys.* **B594** (2001) 272 [[hep-th/0005173](#)].
- [55] P. D. Anderson and M. Kruczenski, *Loop Equations and bootstrap methods in the lattice*, *Nucl. Phys.* **B921** (2017) 702 [[1612.08140](#)].
- [56] H. W. Lin, *Bootstraps to Strings: Solving Random Matrix Models with Positivity*, [2002.08387](#).

- [57] M. Bill, V. Goncalves, E. Lauria and M. Meineri, *Defects in conformal field theory*, *JHEP* **04** (2016) 091 [[1601.02883](#)].
- [58] S. Giombi, R. Roiban and A. A. Tseytlin, *Half-BPS Wilson loop and AdS_2/CFT_1* , *Nucl. Phys.* **B922** (2017) 499 [[1706.00756](#)].
- [59] N. Kiryu and S. Komatsu, *Correlation Functions on the Half-BPS Wilson Loop: Perturbation and Hexagonalization*, *JHEP* **02** (2019) 090 [[1812.04593](#)].
- [60] M. Beccaria, S. Giombi and A. Tseytlin, *Non-supersymmetric Wilson loop in $\mathcal{N} = 4$ SYM and defect 1d CFT*, *JHEP* **03** (2018) 131 [[1712.06874](#)].
- [61] M. Beccaria, S. Giombi and A. A. Tseytlin, *Correlators on non-supersymmetric Wilson line in $\mathcal{N} = 4$ SYM and AdS_2/CFT_1* , *JHEP* **05** (2019) 122 [[1903.04365](#)].
- [62] D. Correa, M. Leoni and S. Luque, *Spin chain integrability in non-supersymmetric Wilson loops*, *JHEP* **12** (2018) 050 [[1810.04643](#)].
- [63] A. Almelid, C. Duhr and E. Gardi, *Three-loop corrections to the soft anomalous dimension in multileg scattering*, *Phys. Rev. Lett.* **117** (2016) 172002 [[1507.00047](#)].
- [64] A. Almelid, C. Duhr, E. Gardi, A. McLeod and C. D. White, *Bootstrapping the QCD soft anomalous dimension*, *JHEP* **09** (2017) 073 [[1706.10162](#)].
- [65] B. Fiol, E. Gerchkovitz and Z. Komargodski, *Exact Bremsstrahlung Function in $N = 2$ Superconformal Field Theories*, *Phys. Rev. Lett.* **116** (2016) 081601 [[1510.01332](#)].
- [66] C. Gomez, A. Mauri and S. Penati, *The Bremsstrahlung function of $\mathcal{N} = 2$ SCQCD*, *JHEP* **03** (2019) 122 [[1811.08437](#)].
- [67] D. Correa, J. Henn, J. Maldacena and A. Sever, *The cusp anomalous dimension at three loops and beyond*, *JHEP* **05** (2012) 098 [[1203.1019](#)].
- [68] M. Kim, N. Kiryu, S. Komatsu and T. Nishimura, *Structure Constants of Defect Changing Operators on the $1/2$ BPS Wilson Loop*, *JHEP* **12** (2017) 055 [[1710.07325](#)].
- [69] A. Cavagli, N. Gromov and F. Levkovich-Maslyuk, *Quantum spectral curve and structure constants in $\mathcal{N} = 4$ SYM: cusps in the ladder limit*, *JHEP* **10** (2018) 060 [[1802.04237](#)].
- [70] D. H. Correa, P. Pisani and A. Rios Fukelman, *Ladder Limit for Correlators of Wilson Loops*, *JHEP* **05** (2018) 168 [[1803.02153](#)].
- [71] D. Correa, P. Pisani, A. Rios Fukelman and K. Zarembo, *Dyson equations for correlators of Wilson loops*, *JHEP* **12** (2018) 100 [[1811.03552](#)].
- [72] J. McGovern, *Scalar Insertions in Cusped Wilson Loops in the Ladders Limit of Planar $N=4$ SYM*, [1912.00499](#).